UNIVERSITY OF CALIFORNIA SAN DIEGO

GLP-1 Effects on Maternal Metabolism and Fetal Development

A Thesis submitted in partial satisfaction of the requirements for the degree Master of Science

in

Biology

by

Cindy V Lu

Committee in charge:

Professor Jianhua Shao, Chair
Professor Randolph Hampton, Co-Chair
Professor Keefe Reuther

2022

The Thesis of Cindy V Lu is approved, and it is acceptable in quality and form for publication on microfilm and electronically.

University of California San Diego

2022

DEDICATION

I would like to dedicate this thesis to my parents who have supported me throughout my education and the opportunity they gave me to complete a postsecondary degree at a prestigious university. Without their efforts, I would not be who I am today.

TABLE OF CONTENTS

LIST OF FIGURES

LIST OF TABLES

ACKNOWLEDGEMENTS

I would like to acknowledge and express my special thanks to my professor and chair of my committee, Jianhua Shao who has supported me and guided me throughout my project. I also would like to thank my defense committee, who provided support and knowledge to me.

Additionally, I would like to give the warmest thanks to Liping Qiao who has helped me throughout my project by assisting with mice handling, harvesting tissue, and other experiments. I am also grateful to Sarah Saget who was also my mentor during the time she was in our lab as a postdoctoral researcher. I would also like to express my gratitude to other students that were in our lab who has assisted with calculations and taking images for me.

Lastly, I would like to thank once again my family who has supported and believed in me to finish my post-secondary education and now, to finish my master's degree. Especially to my grandmother, who is not here with us today but remains in my heart guiding me.

This thesis is currently being prepared for submission for publication. The thesis author was the primary author of this paper with Liping Qiao and Jianhua Shao as co-authors.

ABSTRACT OF THE THESIS

GLP-1 Effects on Maternal Metabolism and Fetal Development

by

Cindy V Lu

Master of Science in Biology

University of California San Diego, 2022

Professor Jianhua Shao, Chair
Professor Randy Hampton, Co-Chair

Glucagon-like peptide-1 (GLP-1) is an incretin hormone that regulates postprandial glucose homeostasis through insulin secretion, food intake, gastric emptying, and suppression of glucagon secretion. As glucose is one of the vital sources of energy for the fetus during fetal

development, the regulation of glucose and its uptake is important. Yet, GLP-1's role in maternal metabolism or fetal development is still unknown. Thus, GLP-1R agonist, Semaglutide, and antagonist, Exendin-9, were injected into mice during late gestation to understand the effect of GLP-1 on maternal metabolism and fetal development. There were no differences in body weight of the dams, food intake, and dam insulin serum levels; however, there was a transient period of reduced glucose serum levels in the GLP-1R agonist. Additionally, the E18.5 fetal weight of the agonist and the antagonist were reduced compared to the control. Interestingly, there was no significant difference between the placenta weights; however, there was a decrease in placenta efficiency in GLP-1 antagonist injected placenta leading to the transient period of increased levels of glucose in the dam after the injection. While the GLP-1R agonist dams had diminished dam serum glucose levels during that period. Furthermore, there was a reduction of angiogenesis in the placenta due to the decrease of labyrinth zone, the area of nutrient exchange between the dam and fetus in both the agonist and antagonist injected placenta. Therefore, GLP-1 in addition to glucose homeostasis may also regulate the endothelial blood vessel by angiogenesis and vessel permeability.

INTRODUCTION

Glucagon-like peptide-1 (GLP-1) is a peptide hormone that has various metabolic effects within the body. These effects include glucose-dependent stimulation of insulin secretion, decrease of gastric emptying, inhibition of food intake, increase of natriuresis and diuresis, and β-cell proliferation (1). Glucagon-like peptide 1 (GLP-1) was first discovered from the cloning of the preproglucagon gene which expedited the study and research of gut endocrine peptide hormones (2-3). After the generation and characterization of the first glucagon-detecting antibody by Roger Unger, the development of radioimmunoassay (RIA) to detect glucagon in blood and tissue samples emerged (4). Additionally, there was confirmation of glucagon-like immunoreactivity present in extra-pancreatic tissues, particularly the intestines (5). With this detection method, Unger further demonstrated in 1968 that intraduodenal glucose administration increases circulating glucagon-like immunoreactivity indicating that the intestines secrete a glucagon-like material (6). GLP-1 originates from the 18-kDa mammalian proglucagon protein from the preproglucagon gene (Gcg) (7). GLP-1 is expressed in the Preproglucagon (PPG) neurons throughout the brain, especially in the nucleus tractus solitarii (NTS) and medullary intermediate reticular nucleus, α-cells from the islet in the pancreas, and throughout the intestines, specifically in L cells (1,8). GLP-1 in the brain, intestines, and pancreas differ by tissue-specific post-translational processing (9-10). In the pancreas, the islet α-cells utilizes prohormone convertase 1/3 (PC1/3) and prohormone convertase 2 (PC2) to cleave the proglucagon protein to bioactive glucagon, GRPP, IP-1, major proglucagon fragment (MPGF), and GLP-1 (11-13). In the intestines and brain, PC1/3 cleaves proglucagon to GLP-1, GLP-2, and oxyntomodulin (7).

GLP-1 plays an important role in glucose homeostasis and enhances glucose-induced insulin secretion while inhibiting glucagon secretion (14-15). In response to food intake, GLP-1

is secreted from L-cells that has direct contact with luminal nutrients through its apical surface (16-19). GLP-1 diffuses across the basal lamina into the lamina propria and finally into the capillaries in the intestine. GLP-1 circulates through the portal system and only 25% reaches the liver while 10 – 15% reaches the global circulation which then passes through the pancreas (20). This is due to the serine protease dipeptidyl peptidase 4 (DPP-4) that cleaves dipeptides from the amino terminus of oligopeptides or proteins that contain an alanine or proline residue in position 2 which modifies or inhibits their activity which causes the half-life of GLP-1 to be less than 2 minutes (17). Furthermore, GLP-1 in the portal system also activates GLP-1Rs in the vagal sensory neurons that communicate with brain stem neurons to regulate metabolism (14,21). Although, a minimal amount of GLP-1 passes through the region, picomolar concentrations of GLP-1 is sufficient to activate the glucagon-like peptide-1 receptors (GLP-1Rs) in the pancreas (22). GLP-1Rs are broadly found in most tissues of the body such as the brainstem, blood vessel, heart, hippocampus, hypothalamus, kidney, lung, pancreatic islets, and stomach (23-26). They are G-protein coupled receptors that are from the B family class which are made up of seven transmembrane heterotrimeric G-protein-coupled receptors that have that a long extracellular N-terminus with an α-helical region, five β-strands that form two antiparallel β-sheets and six conserved cysteine residues (27,28). GLP-1Rs can also activate other G-coupled receptor pathways such as $G_{\alpha i}$, $G_{\alpha o}$, and $G_{\alpha q/11}$ but the prominent pathway is the $G\alpha_s$ which increases the level of cyclic Adenosine Monophosphate (cAMP) through activation of adenylate cyclase (27,29-31). The activation of cAMP upregulates Protein Kinase A (PKA) and exchange protein directly activated by cAMP2 (Epac2) which stimulates voltage dependent Ca2+ channels to open and exocytosis of insulin occurs (30,32). GLP-1 induced activation of PKA also stimulates expression of transcription factor pancreatic duodenal homeobox-1 (PDX-1) that binds to the

insulin promoter to initiate insulin synthesis (18,33-35). Insulin, in turn, regulates blood glucose levels by facilitating cellular glucose uptake, regulating carbohydrate, lipid, and protein metabolism. Insulin also promotes cell division and growth by its mitogenic effects (36). In addition to glucose-dependent stimulation of insulin secretion, GLP-1 also decreases gastric emptying, inhibition of food intake, and inhibition of glucagon secretion (1,15,37-38). Furthermore, the GLP-1 induced rise of insulin mRNA also displayed an increase in GLUT1 and hexokinase1 mRNA expression (33,39). Thus, GLP-1 has a major role in blood glucose homeostasis.

Throughout pregnancy, maternal metabolism changes to accommodate the distribution of nutrients between the mother and the fetus which include the various stages of embryo implantation, fetal and placental development, lactation, and finally for delivery. One of these notorious changes is glucose metabolism. For proper growth and development of the fetus, the nutrient flow from mother to fetus across the placenta must be maintained. A glucose gradient is established during early pregnancy by fetal β – cells by maintaining a low glucose levels in fetal circulation since glucose transport is a passive process and requires facilitation by glucose transporters (40-41). In the later stages of pregnancy, the overflow of glucose circulation from the maternal circulation causes a shift in the gradient established by the fetus and to counter this, placenta releases hormones to increase maternal insulin resistance and hepatic glucose production (42-43). To compensate for the maternal insulin resistance, β – cells in the pancreas expand their mass and proliferate to increase insulin circulation (44-45). Interestingly, although there is pregnancy induced insulin resistance within tissues (46), maternal blood concentrations of glucose are reduced because of the surge of glucose consumption in the placenta for fetal

development (46-50). Thus, the adaptations in metabolism during pregnancy consists of elevating maternal blood insulin and diminished maternal blood glucose concentrations.

Incretin hormones like GLP-1 have been suggested to have a role in maternal metabolism and fetal growth. This is due to the GLP-1's major role in glucose homeostasis and its influence over β – cells. Furthermore, in pregnant GLP-1R KO mice, there was no increase in islet or β – cell area compared to the C57BL/6 mice leading to the proposition that perhaps GLP-1 may affect the β – cell expansion during pregnancy (51). Multiple studies have indicated there was reduced levels of serum GLP-1 during pregnancy (52-55). Researchers have also studied the effects of GLP-1R agonists during pregnancy. In rats, there was a potential direct effect of Semaglutide, a GLP-1R agonist, in the later stages of pregnancies (56). It was also reported that there was reduced fetal weight in rats from rats that had injections of the agonists towards late pregnancy (56). Furthermore, in mice there was also a similar study on long-term functional alterations following prenatal GLP-1R activation utilizing Exendin-4, another GLP-1R agonist, that resulted in increase in offspring weight (57). Thus, the precise role of GLP-1 on pregnancy is still ambiguous.

Given the importance of GLP-1 in glucose homeostasis by its regulation of insulin, GLP-1 could play a role in maternal metabolism and fetal growth during pregnancy. Pregnancy induces the body to be in an insulin resistant state and advances insulin resistance as gestation continues (58). Therefore, the aim of this study is to determine the effect of GLP-1 on maternal metabolism and fetal development. GLP-1R agonist, Semaglutide, and GLP-1R antagonist, Exendin-9 were injected in C57BL/6 mice during the late pregnancy period. The dam tissues, fetus tissues, placenta, dam serum, fetal serum, and placenta were collected at E18.5 during the end of pregnancy.

MATERIALS AND METHODS

The anti-glucagon antibody was from R&D System (Minneapolis, MN). Antibodies against Insulin, CD31 and Ki67 were from Abcam (Cambridge, MA). The total GLP-1 ELISA kit, IGF-1 ELISA kit, TRIzol, NuPAGE Gels, SuperScript III Reverse Transcriptase and Oligo $(Dt)_{12\text{-}18}$ Primer, Alexa-Fluor-conjugated goat anti-mouse, and rabbit antibodies were from Invitrogen (Carlsbad, CA). Glucose, glucose oxidase, Exendin-9, BSA, and Schiff Reagent were from Sigma-Aldrich (St. Louis, MO). The mouse insulin ELISA kit was from Mercodia (Uppsala, Sweden). TG assay kit was from Pointe Scientific, Inc (Canton, MI). NBT/BCIP Stock solution was from Roche Diagnostics (Indianapolis, IN). Super Signal West Pico PLUS Chemiluminescent Substrate was from Thermofischer scientific (Waltham, Massachusetts). Semaglutide (Sem) was obtained from Novo Nordisk (Plainsboro, NJ). Exendin-9 (Ex9) was from Med Chem Express (Monmouth Junction, NJ).

Mice

The mice were C57BL/6 mice from the Jackson Laboratory (Bar Harbor, ME). The female mice started mating after eight to ten weeks after birth. Pregnancy was determined by the vaginal plug and assigned the embryonic age E (0.5). The dams were then subcutaneously injected with the various treatments randomly: Saline (control), Semaglutide (GLP-1R agonist) with varying dosages of 6µg/kg and 12µg/kg, and Exendin-9 (GLP-1R antagonist, 15 µg). The dams were injected in the morning of E13.5, E15.5, and E17.5 and were also monitored for maternal body composition by EchoMRI. Maternal tissue, placenta, and pup tissue were harvested at E18.5. Experiments using mouse models were carried out under the Association for

Assessment and Accreditation of Laboratory Animal Care guidelines with approval from the University of California San Diego Animal Care and Use Committee.

Immunohistochemistry

The tissues were fixed in either in 4% paraformaldehyde or 10% neutral-buffered formalin and then embedded in optimal cutting temperature compound (O.C.T.) or paraffin, respectively. For Immunohistochemistry (IHC), the slides were blocked in 2% H_2O_2 for 10 minutes and then either heated to 95°C in a water bath for 10 minutes (Glucagon) 30 minutes (CD31) for antigen retrieval in 0.1M Citrate Buffer Ph 6.0. For insulin, the antigen retrieval was done with PBS 1% SDS buffer for 5 minutes in room temperature. The slides were blocked for 2 hours at room temperature in a humid chamber with blocking buffer. After that, the slides were put in primary antibody overnight at 4°C: Glucagon (1:200), CD31 (1:500), Insulin (1:100) and the controls (negative) were put in blocking buffer. After washing, the slides were put in secondary antibody (1:200) goat anti-rabbit from Cell Signaling for 2 hours at room temperature in a humid chamber. The signal was visualized with 3,3′-diaminobenzidine (Vector Laboratories, Burlingame, CA) at room temperature for 10 minutes (Glucagon and Insulin), 30 minutes (CD31) and counterstained with hematoxylin. The images for IHC and IF were done on the BZ-X800E Keyence microscope. The α-cells, β-cells, and pancreas area, Capillary Area Density (CAD), Capillary Number Density (CND), Capillary Surface Density (CSD), and Area per Capillary (APC) were measured with ImageJ.

For immunofluorescence (IF), the slides were put in PBS 1% SDS for 5 minutes for antigen retrieval and then incubated at room temperature for 2 hours in a humid chamber with blocking buffer. The slides were then stained with primary antibody: Glucagon (1:200), Insulin (1:100), Ki67 (1:100), and CD31 (1:500) overnight at 4°C. After washing, the slides were put in

the secondary antibody conjugated with Alexa Fluor 488 or 568 was applied to the slides and incubated for 2 hours at room temperature. The slides were then washed, and sections were mounted in DAPI Fluoromount-G (Southern Biotech, Birmingham, AL). The slides were visualized by fluorescent optical microscopy with BZ-X800E Keyence microscope. The ratios of Ki67 and glucagon or insulin protein–positive cells were calculated with use of IF images. The CD31 ratio to the labyrinth area were also calculated with the IF images in ImageJ.

Staining

Placentas were fixed in paraffin were stained with Periodic-Acid Schiff (PAS). The paraffin slides were deparaffinized and rehydrated before staining, The slides were placed in 0.5% periodic acid solution for 5 minutes and then rinsed in distilled water. After that, the slides were placed in Schiff reagent for 20 minutes and washed with lukewarm water for 5 minutes. The slides were counterstained with hematoxylin.

Placentas that were fixed in paraffin or O.C.T. were stained with Endogenous Alkaline Phosphatase (AP). All paraffin slides must be deparaffinized and rehydrated before staining. The placenta slides were put in NTMT solution 2 times for 10 minutes. The slides were then stained with the NBT/BCIP solution in the dark for 20 minutes and counterstained with Nuclear Fast Red. These slides were used to calculate the cross-sectional area of the placenta using ImageJ.

Assays

ELISA mouse IGF-1 kit from Invitrogen. The samples must be pre-diluted before adding to the assay. The serum was diluted 1:5 fold and diluent A should be used for dilution of the serum. To dilute the standards, first briefly spin down the vial and then add 400 µl of assay diluent A. Dissolve thoroughly and add 20 µL of IGF-1 standard vial to prepare a 100 ng/mL

standard into a tube of 980 µL assay diluent A to prepare a 2,000 pg/mL standard solution. Use the 2,00 pg/mL standard solution to produce a dilution series that results in standards of 666.7 pg/mL, 222.2 pg/mL, 74.07 pg/mL, 24.69 pg/mL, 8.23 pg/mL, and 2.74 pg/mL. Diluent A will serve as the blank. Add 100 µL of standards to the appropriate wells and add 100 µL of diluted samples to the wells. Cover the wells and incubate overnight at 4°C with gentle shaking. The next day prepare 1x wash buffer from 20x wash concentrate by diluting 20 mL of the concentrate into 380 mL of deionized water. Prepare biotin conjugate before use and add 100 µl of 1x Assay Diluent B into the vial with biotin conjugate concentrate. Diluent B is diluted 20 - fold with deionized water before use. Pipette and mix gently, the biotin concentrate should be diluted 80-fold with 1X assay diluent B. Then wash the wells 4 times with the 1x wash buffer with 300 µL of wash buffer per well. After the last wash, remove any remaining wash buffer by aspirating and invert the plate against clean paper towels. Add 100 µL of biotin conjugate and incubate for 1 hour at room temperature with gentle shaking. Discard the solution and repeat the washing step. Prepare the 1x Streptavidin-HRP solution 15 minutes before usage by briefly spinning and mixing gently before use. Dilute the streptavidin-HRP 200-fold with 1x Assay diluent B. Add 100 µL of prepared streptavidin-HRP solution and incubate for 45 minutes at room temperature with gentle shaking. Discard the solution and repeat the washing step again. Add 100 µL of TMB substrate to each well and incubate for 30 minutes at rom temperature in the dark with gentle shaking. Add 50 µL of stop solution to each well and tap the side of the plate to gently mix. Read and generate the standard curve on the plate reader. The absorbance should be at 450 nm.

Mouse insulin ELISA kit from Mercodia. Prepare 1x enzyme conjugate solution by diluting with the 11x enzyme conjugate buffer. Prepare the 1x wash buffer solution by diluting

21x in distilled water. Prepare the microplate wells to include the calibrators, controls, and samples in duplicates. Pipette 10 µL each of calibrators, controls, and samples into the wells. Add 100 µL of enzyme conjugate 1x solution into each well. Incubate for 2 hours at room temperature on a plate shaker. After that, wash the plate 6 times with 700 µL of wash buffer 1x solution per well. After the final wash, invert and tap the plate firmly against a clean paper towel. Add 200 µL of substrate TMB into each well and incubate for 15 minutes at room temperature. Add 50 µL of stop solution to each well and place on plate shaker for a few seconds to ensure mixing. The plate is then read at 450 nm on a plate reader.

Glucose measurements are done with the PGO enzyme and O-Dianisidine tablets. The mix solution is prepared by 400 µL of O-Dianisidine to 25 mL of PGO. Then pipette 200 µL of the mix into each well. Next, pipette 1 µL of each standard, control, and sample into the wells. Place the plate on the plate shaker to briefly mix. Cover microplate with a plate sealer and incubate for 30 minutes at 37°C. Remove any bubbles that are within the wells and then read the plate.

Western Blot and Real-time PCR assays

Protein samples were extracted from tissue and then homogenized in lysis buffer for 5 minutes. The homogenized tissue is then spun in the centrifuge for 20 to 30 minutes at 5000 RPM in the 4 °C room. The protein was then transferred into a centrifuge tube and put in the centrifuge for 30 minutes at high speed in the 4 °C room. The protein was centrifuged and transferred again if there are still impurities in the sample. After that, protein concentration was calculated. The BioRad Protein assay was used. Add 200 µL of the protein assay to each well and add 1 µL of your standards and samples to the wells. Briefly shake the plate on the plate shaker to mix and remove any bubbles that are formed. The plate is then read on the plate reader.

Depending on what tissue type, the amount of volume of the protein added to the western blot will be calcualted. The protein sample are then prepared for the western blot by adding the amount of volume needed and the loading buffer. The samples are then heated om a heat block for 10 minutes at 160°C. The samples are now ready to be added to the SDS-PAGE gels. The gel we use to run the western blot is made in our lab. We first make the 10% SDS-PAGE gel and then the 10% stacking gel. The combs are then added after a layer of isopropanol is added to even out the stacking gel. The protein samples and protein ladder were then added into the 10% SDS-PAGE gels with the running buffer which consists of tris, glycine, and SDS at pH 8.3. The gel was then ran using the BioRad wet blotting box at 100V during the first 10 minutes until all the protein has passed through the stacking gel. Then it was run at 140V until it reached the bottom of the gel. After that the gels are placed with a PVDF membrane in a BioRad wet blotting box with the transfer buffer. The transfer buffer consists of tris, glycine, at pH 8.3 with 20% methanol. The transfer is then run at 100V for 2 hours. After this, the western blot membrane is put into blocking buffer for 1 hour on the shaker. Then the membrane was put in a primary solution at 4°C overnight. Horse-radish peroxidase-linked secondary antibodies were from Santa Cruz Biotechnology and Cell Signaling. Super Signal West Pico PLUS chemiluminescence substrate was used to visualize the bands. Quantity One software (Bio-Rad Laboratories) was used to calculate the band densities.

Total RNA extraction was prepared from tissues with TRIzol and then homogenizing the tissue. Then, it was centrifuged for 10 minutes at 600xg in the 4° room. The supernatant was then added into a new centrifuge tube. Then, Chloroform was added. Mix the solution gently and then centrifuge for 15 minutes at 11,000xg. Transfer the supernatant into a new tube and add isopropanol. Mix gently and centrifuge again for 10 minutes at 11,000xg. Then wash the pellet

with 70% ethanol with DEPC water. Then centrifuge for 5 mins at 7500xg and remove all the supernatant and keep the pellet. Add deionized water and heat the RNA at 10 minutes at a heating block at 60°C. After that, the RNA concentration is calcualted by adding 200 µL of PCR water into each centrifuge tube and 1 µL of sample to the water and mix. The mix is then added to the RNA cuvette and concentration is measured by the Spectrophotometer (Biophotometer). The OD should be around 1.5 to 2 to have the best amount of purity. The RNA is now ready for cDNA synthesis. cDNA was synthesized with SuperScript III Reverse Transcriptase, Oligo $(Dt)_{12\text{-}18}$ Primer, 10x Buffer, 100 mM DTT, dNTP, and RT enzyme. The PCR was then run at (enter the program). After that Real-Time PCR was performed with QuantStudio 3 Real-Time PCR System (Invitrogen) and specific primers (Table 1). Expression data was normalized to the amount of 18s Rrna.

Statistical Analysis

Data are expressed as mean ± SEM. Statistical analyses were performed with the student *t* test or ANOVA, followed by Bonferroni posttests with the use of Prism software. Differences were considered significant at $P < 0.05$.

Table 1. Sequences for real-time PCR primers

Gene	Forward (5' to 3')	Reverse (5' to 3')
18S rRNA	CGAAAGCATTTGCCAAGAAT	AGTCGGCATCGTTTATGGTC
Angpt1	CAGTGGCTGCAAAAACTTGAGA	GGCCGTGTGGTTTTGAACAG
mFABPpm	ATCTGGAGGTCCCATTTCAA	ATGGCTGCTGCCTTTCAC
Glut1	GACCCTGCACCTCATTGG	GATGCTCAGATAGGACATCCAAG
Lat1	CAAAGTGCCAAGAAAAAGAGC	CTGAGCAGGGAGGAACCAC
Snat1	CTTCAGCCATAAAATCCCTCAT	CATCGACGTACCAGGCTGA
Snat2	CAATGAGATCCGTGCAAAAG	TGCTTCCAATCATCACCACT
Vegfa	CGGGCCTCGGTTCCA	GCAGCCTGGGACCACTTG
Vegfr1	GAAGGAACAAATAAGATGTGCCG	TGTCCGTAGCAGAATCCAGG

RESULTS

The C57BL/6 dams were injected with Saline, Sem, Sem HD, or Ex9 during late pregnancy at E13.5, E15.5, and E17.5. During these time points, the dams were scanned by the EchoMRI the only exception was the Ex9 dams. There was no significant difference in the body weight, fat, lean fat, percent fat, and percent lean fat from the EchoMRI scans compared to the control. The dam and pups were then harvested at E18.5 with their blood, tissues, weight, placenta weight. There was a significant decrease in E18.5 fetal weight compared to the control for the three treatments (Figure 1). The most significant decrease was in the Ex9 fetal weight ($P<0.0001$). There was no significant difference between the Sem dosages; however, there was a slight decrease ($P = 0.069$). The male fetal weight displayed a decrease in body weight between the control and Sem dosage treatment with Semaglutide high dosage with the significant decrease ($P< 0.0007$) and low dosage ($P<0.04$). There was a decrease in the male fetal body weight from the Ex9 injected dams but there was no significant difference ($P=0.0524$). Interestingly, in the female fetal weight the only significant difference was found in the Ex9 treatment ($P<0.0007$). Although, there is a decrease trend that is also shown in the Sem high dosage treatment ($P=0.1$). Additionally, there was no significant difference in the placenta weight between the control and the treatments (Figure 2). The placenta efficiency was also calculated by dividing the fetal body weight to the placenta weight. There was only a significant difference between the control and Ex9 treated placenta ($P<0.003$). Additionally, the placentae from male pups had no significant difference between the treatments while the female pups had a significant difference with the Ex9 placentas ($P<0.03$). Since there was a decrease in the fetal weight and no significant difference in the placenta weight, this led to the investigation to see if there was a maternal effect on the fetus from the injection.

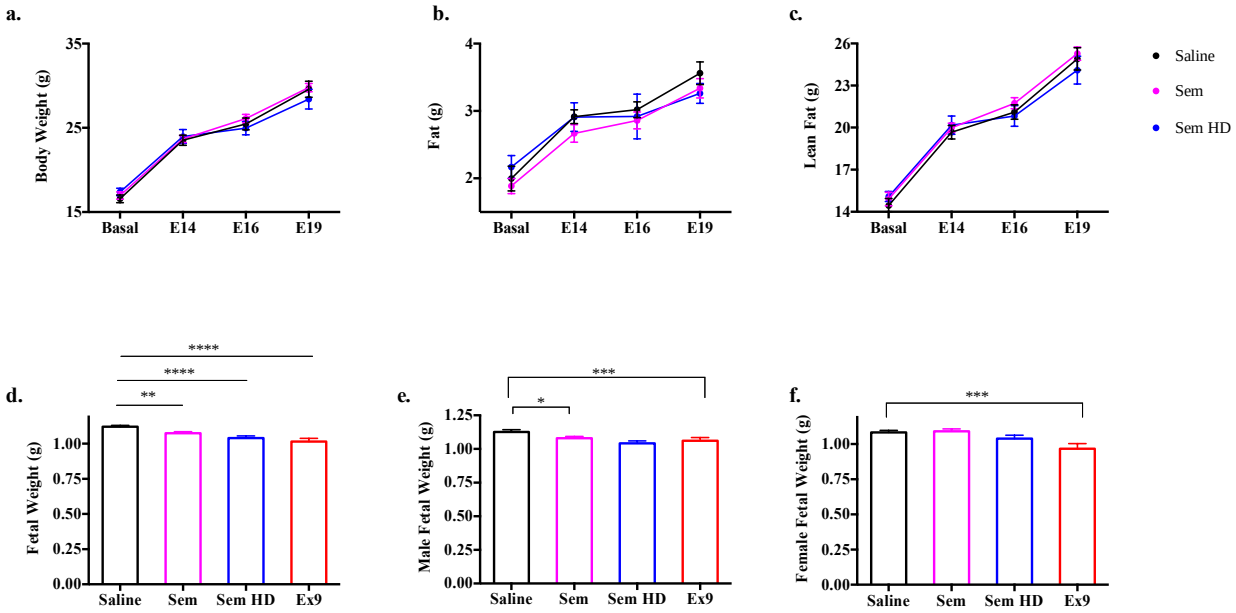

Figure 1. **Reduced C57BL/6 fetal weight of E18.5 dam treated Sem, Sem HD, and Ex9 compared to Saline.** C57BL/6 dams were treated with Saline, Sem, Sem HD, and Ex9 during late pregancy with injections during E13.5, E15.5, and E17.5. Fetal weight was taken at E18.5. There was no significant difference in the EchoMRI scans for (a) body weight, (b) fat, and (c) lean fat. (d) Fetal weight was reduced in all the treatments. Sem ($p<0.002$), Sem HD ($p<0.0001$), Ex9 ($p<0.0001$) decrease compared to Saline. (e) Male fetal weight decreased in Sem dosages. Sem ($p<0.04$) and Sem HD ($p<0.0007$) observed decrease compared to Saline. (f) Female fetal weight decreased in Ex9 treatment only. Ex9 ($p<0.0007$) decrease compared to Saline. All weights were obtained by an analytical scale. Saline (N=17) dams, Sem (N=13) dams, Sem HD (N=13) dams, and Ex9 (N=5) dams.

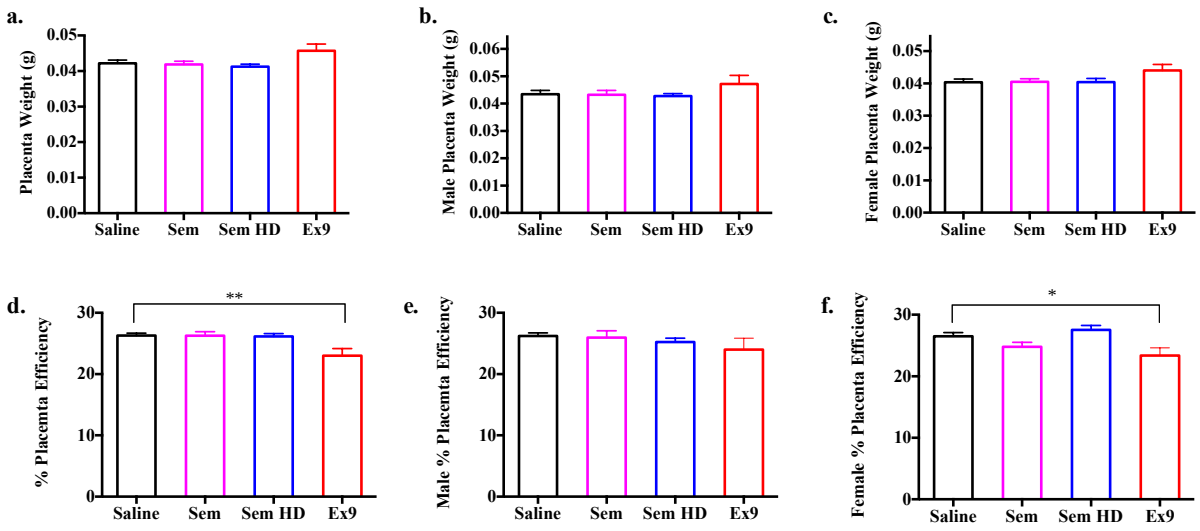

Figure 2. No difference in placenta weight of C57BL/6 dam treated Saline, Sem, Sem HD, Ex9; however, there is a decrease in placenta efficiency in Ex9 treated dams, especially in the female placentas. (a) No significant changes of placenta weight were observed in the treatments compared to saline treated dams. (b) No differences between the treatments for the male placenta weight (c) same is for the female placenta weight. (d) The placenta efficiency ratio that was calculated by taking the body weight divided by the placenta weight displayed a decrease in the Ex9 treated dams ($p<0.003$). (e) Interestingly, there is no significant difference between the treatments and the placenta efficiency for the male ($p=0.1$); however, (f) the female had the significant difference in the placenta efficiency ($p<0.03$). All weights were obtained by an analytical scale.

The availability of resources of energy for the fetus are vital for the potential growth of the fetus. The food intake during the injections and late pregnancy displayed no significant difference in Sem and Sem HD compared to saline. Additionally, there are studies that also show no difference in food consumption (57). Glucose levels indicate the available vital source of energy for fetal development and the affect that the injections had on the dams. The maternal fed E18.5 glucose serum had no significant difference between the treatments and the control (Figure 3). Since there is no change in fed serum glucose, the availability of glucose is most likely not the cause of the fetal weight decrease. Although, there is no overall difference after the three injections of the agonist or antagonist for glucose levels there is a significant difference after each injection which can be seen by the significant decrease of the area under the curve (AUC) of the E15.5 fed interval glucose serum (Figure 4). Indicating that terminally after all the treatments, there was no significant difference; however, there was an effect when the agonist or antagonist was initially injected. Furthermore, the maternal fed E18.5 insulin serum had no significant difference between the treatments and the control (Figure 3). Despite having an increase in insulin levels in the E15.5 fed interval serum there is no significant difference in the AUC (Figure 4). This contrasts the β – cell area ratio compared to the total area of the pancreas where there is an increase between the control and Sem high dosage ($P<0.02$) (Figure 5). Although, there is also no significant difference for the Sem low dosage and Ex9 groups for β – cell area ratio. Thus, indicating that there is additional β – cell area expansion when GLP-1R agonist are injected to the pregnant mice. On the other hand, the α – cell area ratio there is a decrease trend in the area for all treatments (Figure 5); however, the only significant difference was found in the Exendin-9 injected dams ($P<0.018$). Further investigation is needed to determine the mechanism behind the decrease in α – cell area; however, it does indicate that

there is a decrease of glucagon that may be due to the agonist or antagonist. Overall, there is an observed transient decrease in the glucose levels after injection of the agonist; therefore, reduction of fetal weight could be the result of the injection.

Due to the transient reduced levels of glucose, there was also an observed decrease in E18.5 fetal glucose and insulin serum levels in Sem HD and Ex9 treatments (Figure 3). The reduced insulin serum levels made the fetus in an insulin deficient state which caused the decline of potential fetal growth (59,60). Fetal insulin deficiency may be due to the deficiency in nutrients, the production of insulin in the β – cell, or reduced sensitivity to insulin in tissues by their receptors (59). Thus, the western blots were done to determine the sensitivity of insulin within the tissues. The western blot of the E18.5 fetal liver displayed an increase in the insulin receptor between the saline and Sem treated dams ($P<0.0002$) (Figure 6). Furthermore, there was a significant decrease in Sem HD band density ($P<0.03$) in E18.5 fetal liver (Figure 6). Interestingly, p-GSK3 had a significant increase of band density between Sem ($P<0.04$) and Sem HD ($P<0.0007$) compared to Saline in E18.5 fetal skeletal muscle (Figure 6). Therefore, the increase of p-GSK3 in the western blot band density which is known to induce insulin resistance by the phosphorylation of insulin receptor substrate – 1 (IRS1) (61) may lead to the reduced sensitivity to insulin causing the reduced fetal growth.

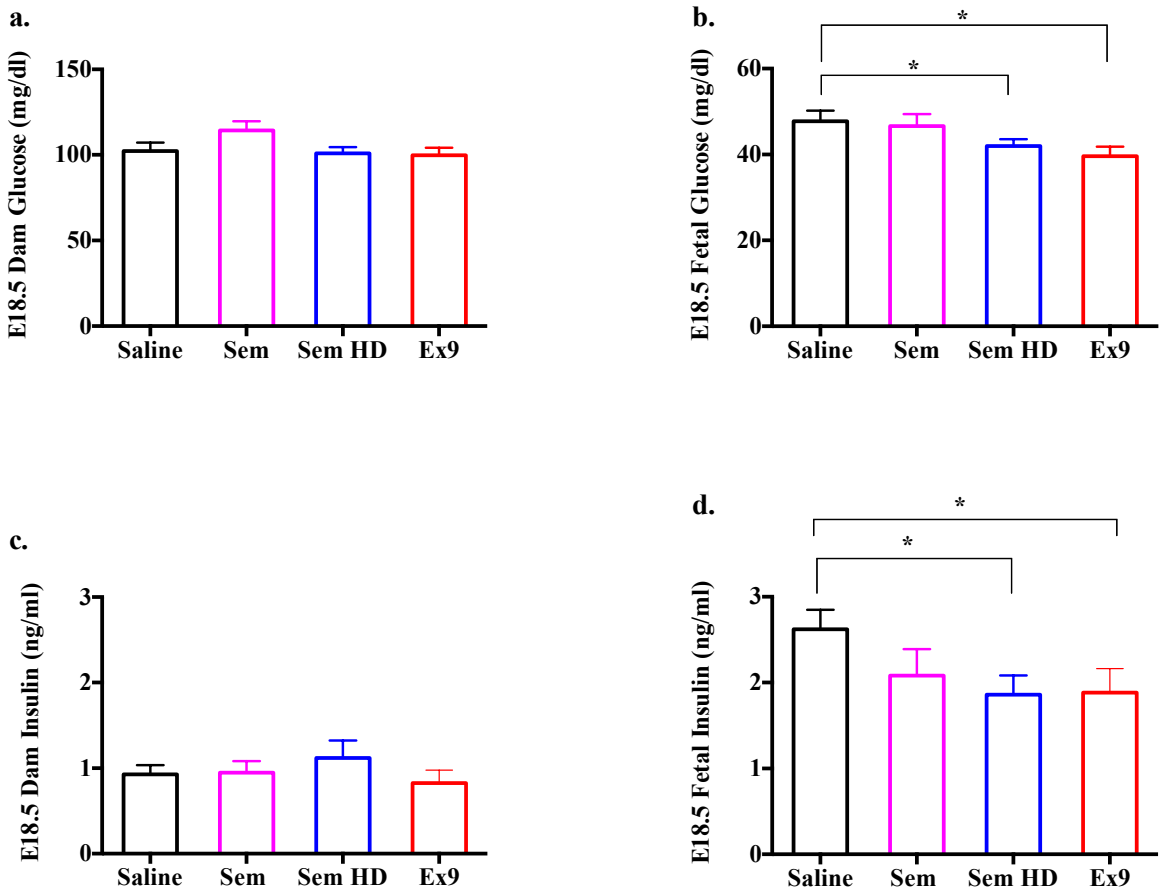

Figure 3. Glucose and Insulin serum levels for E18.5 dam and fetal for Saline, Sem, Sem HD, and Ex9 treatments. E18.5 dam glucose and insulin serum levels were measured. Glucose serum levels for E18.5 dam glucose serum (a) and E18.5 dam insulin serum levels (c) had no significant difference between the treatments. (b) E18.5 fetal glucose serum levels had significant difference in the Sem HD ($P<0.05$) and Ex9 ($P<0.02$) compared to the saline fetal glucose serum levels. (d) E18.5 fetal insulin serum levels had a significant difference in Sem HD ($P<0.02$) and Ex9 ($P<0.05$) compared to the saline control insulin serum levels.

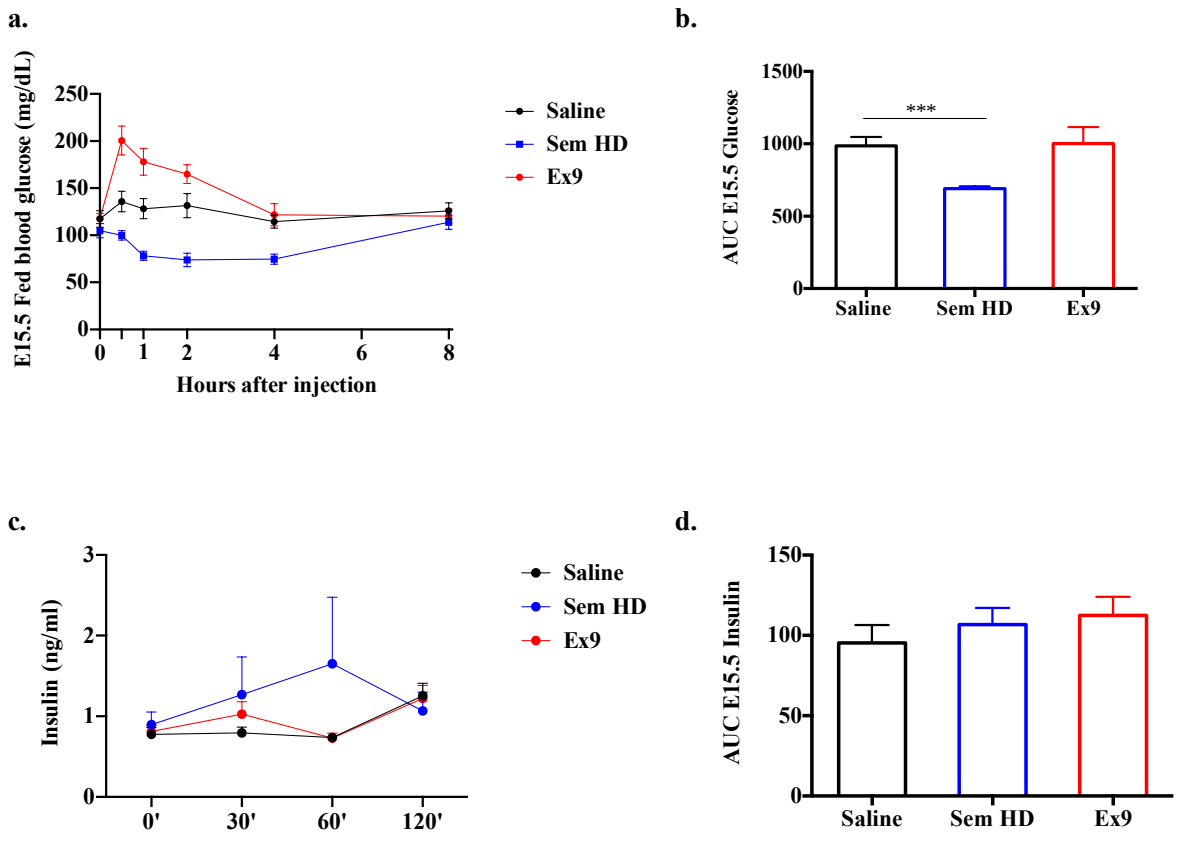

Figure 4. E15.5 glucose and insulin levels after the second day of injection. After the subcutaneous injection of the agonist or antagonist, serum samples were taken from the dam. (a) There was a decrease in the Sem HD injected dam glucose levels and an increase in the Ex9 injected dam glucose levels compared to the control (saline). (b) The AUC of the E15.5 fed glucose serum levels with the AUC defined with arbitrary units had a significant decrease in Sem HD injected dams AUC ($P<0.0007$). The Ex9 injected dam glucose AUC had no significant difference in the increase of AUC compared to the control. (c) The E15.5 fed dam insulin levels had an increase in the Sem HD and Ex9 had no difference in the insulin levels at that time. (d) The AUC of the E15.5 fed insulin had no significant difference in both treatments.

Figure 5. E18.5 dam and pups' pancreas β – cell ratio and α – cell ratio. α – cell and β – cell ratio was calculated by IHC of glucagon and insulin, respectively. The ratios were calculated by dividing the area of glucagon or insulin by the total area of the pancreas. The areas were calculated by ImageJ. (a) Increased ratio of Sem HD β – cell ratio compared to Saline ($P<0.03$) and (b) decreased Ex9 α – cell ratio compared to Saline ($P<0.02$). (d) Images of the representative islets that showcase the increase in β – cell area ratio and the decrease in the α – cell ratio. (e) No significant difference between the β – cell ratio in E18.5 fetal pancreas. (f) Decrease in E18.5 fetal pancreas α – cell ratio for Sem ($P<0.02$), Sem HD ($P<0.05$), and Ex9 ($P<0.002$) compared to Saline.

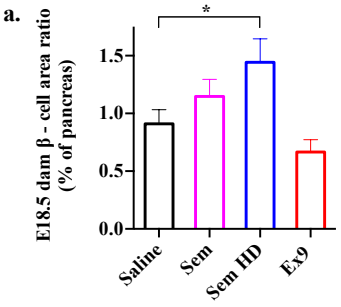
a.
E18.5 dam β - cell area ratio (% of pancreas)
1.5
1.0
0.5
0.0
*
Saline
Sem
Sem HD
Ex9

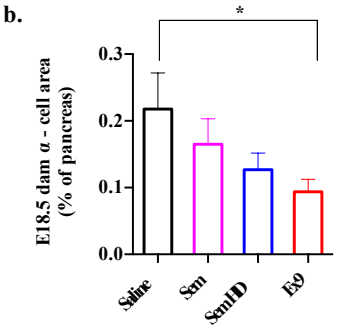
b.
E18.5 dam α - cell area (% of pancreas)
0.3
0.2
0.1
0.0
*
Saline
Sem
SemHD
Ex9

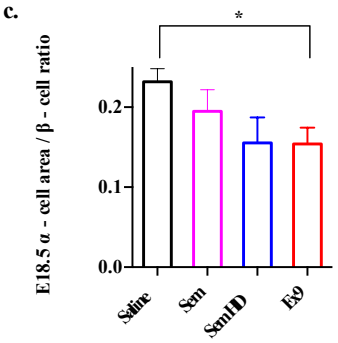
c.
E18.5 α - cell area / β - cell ratio
0.2
0.1
0.0
*
Saline
Sem
SemHD
Ex9

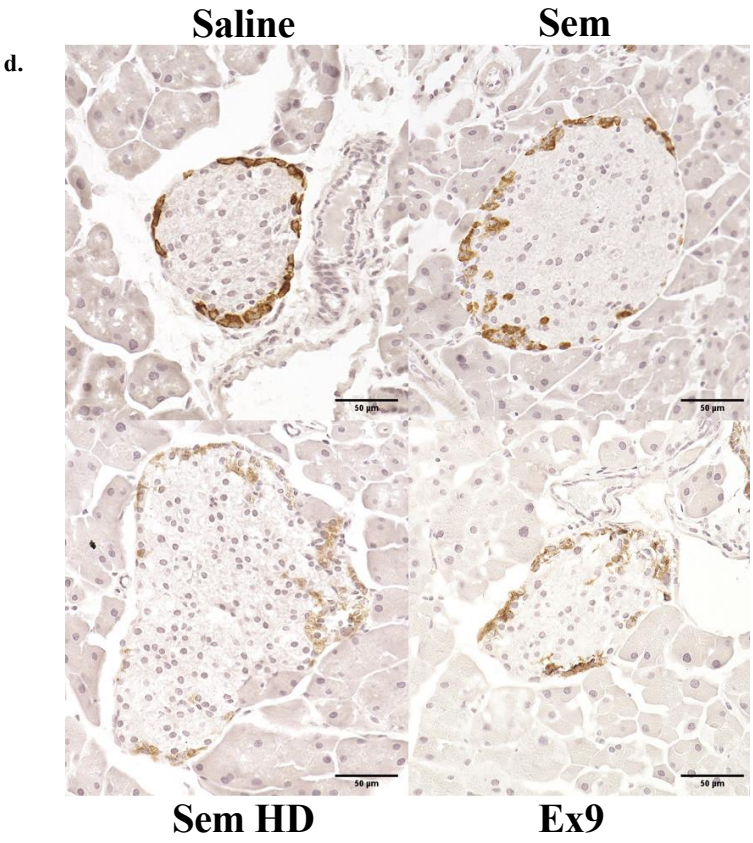
d.
Saline
Sem
Sem HD
Ex9
50 µm

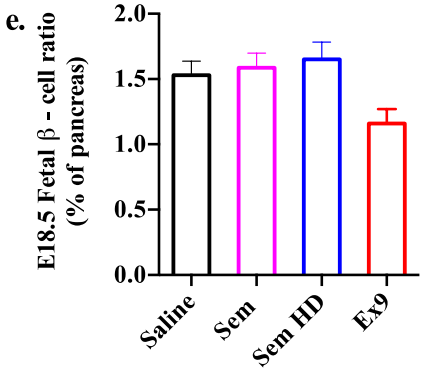
e.
E18.5 Fetal β - cell ratio (% of pancreas)
2.0
1.5
1.0
0.5
0.0
Saline
Sem
Sem HD
Ex9

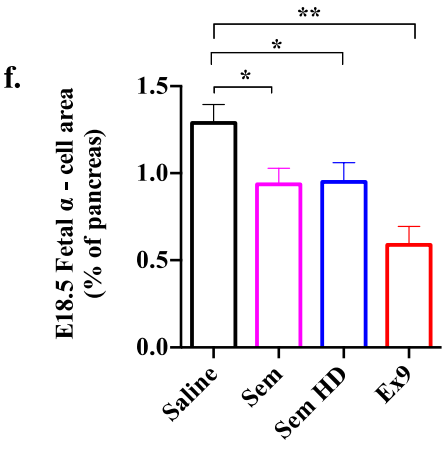
f.
E18.5 Fetal α - cell area (% of pancreas)
1.5
1.0
0.5
0.0
**
*
*
Saline
Sem
Sem HD
Ex9

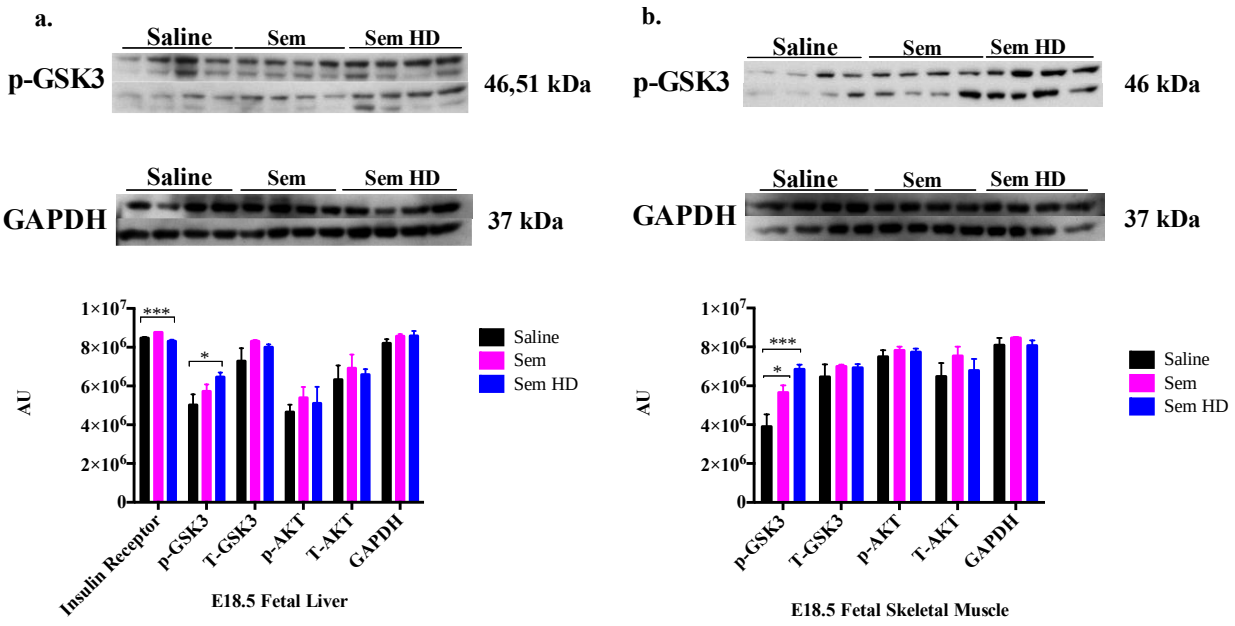

Figure 6. Western Blot of E18.5 fetal liver and skeletal muscle. There is a significant increase of p-GSK3 between saline and the Sem treated fetal liver and skeletal muscle. This increase highlights the increase of insulin resistance within the fetus tissues. Band intensity was calculated using Quantity One (BioRad laboratories software) and the band density has arbitrary unit (AU). (a) In the E18.5 fetal liver there was a significant decrease in Sem HD insulin receptor band intensity ($P<0.0002$) and increase in p-GSK3 band intensity ($P<0.03$). (b) In the E18.5 skeletal muscle there was a significant increase in p-GSK3 band intensity for Sem and Sem HD compared to saline protein.

Other than maternal nutrients, another important factor to look upon in fetal development is the growth factors themselves. The most prominent is the insulin/insulin-like growth factor (IGF) system which regulates fetal and placental growth and development (62). Insulin-like growth factor 1 (IGF-1) and insulin-like growth factor 2 (IGF-2) are the important growth factors in fetal development promoting fetal growth (62). The fetus and the placenta both synthesize them, and IGF-1 specifically is present in syncytiotrophoblast (epithelial covering of the highly vascular embryonic placental villi) and cytotrophoblast (interior layer of the trophoblast) at all stages of gestation (62). Additionally, the significantly decreased levels of insulin can cause the reduction of fetal growth by decreasing the nutrient uptake and the altering the circulation of the insulin-like growth factors (59). Interestingly, the IGF-1 ELISA assay showcased an increase in the fetal serum of the Sem low dosage compared to the control ($P<0.0005$) (Figure 7). There is no significant difference between the Sem high dosage and the Ex9 injected dam E18.5 fetal serum. The E18.5 fetal serum Insulin-like Growth Factor Binding Protein – 1 (IGFBP1) had a decrease in both Ex9 and Sem high dosage treatments; however, the decrease was not significant ($P=0.06$) (Figure 7). IGFBP-1 serves as a binding protein to the IGFs and sequester them from receptor binding but also prolongs the half-life of circulating the blood (62). With the decrease in IGFBP-1, there is less IGFs available to promote growth. Furthermore, there was a decrease in the E18.5 fetal insulin serum levels compared to the Sem high dosage and Ex9 to the control ($P<0.02$ and $P<0.047$, respectively) (Figure 3). Intriguingly, the E18.5 fetal serum also had decrease levels in glucose levels in Sem HD and Ex9 compared to the control ($P<0.05$ and $P<0.02$, respectively) (Figure 3). Therefore, there must be a decrease in nutrient uptake in the placenta rather than the circulations of IGFs that caused the reduction of the fetal weight.

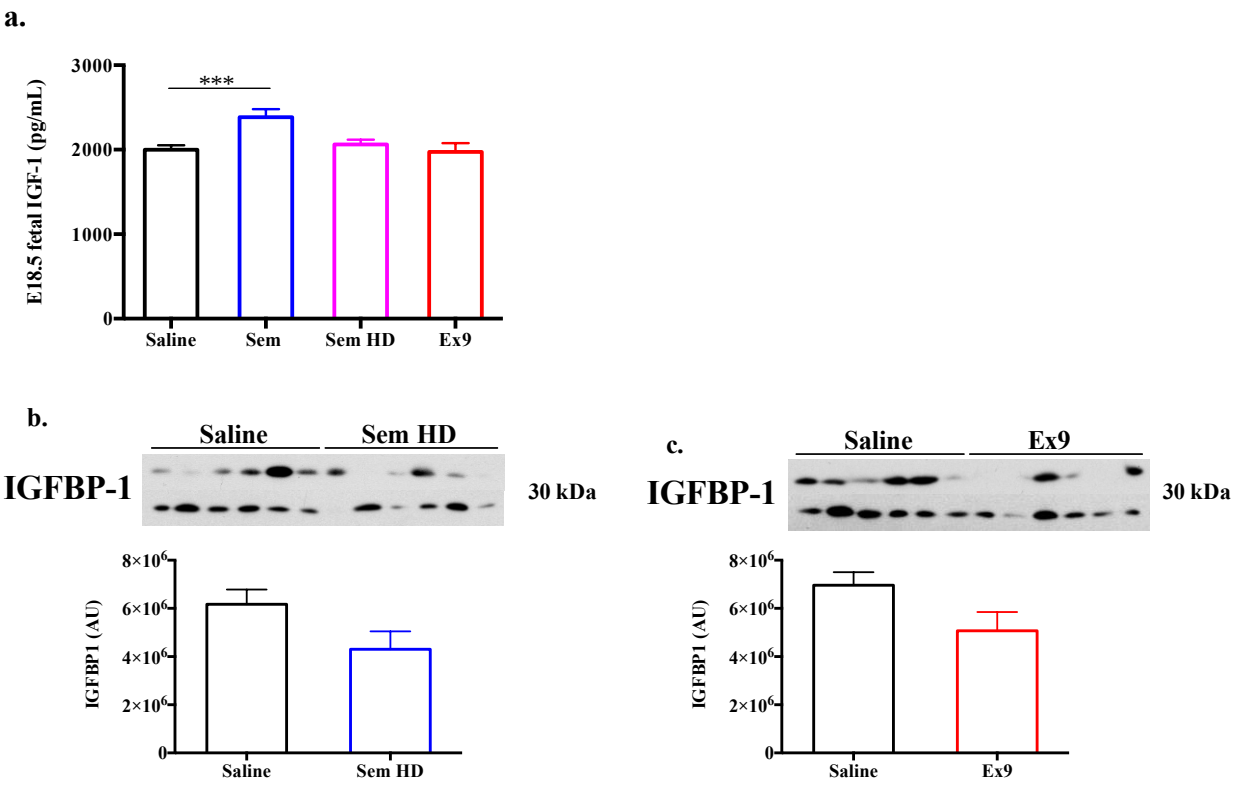

Figure 7. Increase in serum IGF-1 levels in GLP-1R agonist and decrease in serum IGFBP-1. (a). E18.5 fetal IGF-1 levels were measured using an ELISA IGF-1 kit. The E18.5 fetal IGF-1 levels had a significant difference in Sem ($P<0.0005$) compared to saline (control). The IGFBP-1 protein levels for Sem HD (b) and Ex9 (c) were measured by Western Blot and had no significant difference compared to saline (N=6).

In addition to the decreased glucose levels, there might also be a physical difference in the tissue itself where the nutrients and oxygen are being exchanged, the placenta. The mouse placenta has three different zones: the decidua, (DC), the junctional zone (JZ), and the labyrinth (LB) zone (46). The cross-sectional area ratio of the placenta was calculated by manually sectioning the placenta between the different zones: junctional, labyrinth, and decidua from the Alkaline Phosphatase (AP) stain. There was a significant decrease in the LB ($P<0.003$) between the control and Sem placenta while the JZ cross sectional area ratio also exhibited an increase in the area ($P<0.006$) (Figure 8). The Sem HD also exhibits a decrease in LB cross sectional area; however, the decrease is not significant ($P=0.06$) (Figure 8). Additionally, the JZ for Sem HD also had an increase in area but the difference between the controls was not significant ($P=0.2$) (Figure 8). A small LB area indicates a reduced transport area for nutrients to reach the fetus, and eventually restricting fetal growth (63). Thus, the reduction in the LB area of the Sem and Sem HD may lead to the decrease in fetal weight as there is less nutrients transferring to the fetus. JZ has been known for its endocrine function within the placenta and the storage of glycogen (64). Interestingly, there was an increase in the Periodic-Acid-Schiff (PAS) stain, which is known to stain polysaccharides (glycogen) and mucosubstances (glycolipids and glycoproteins) (64) in the Sem and Sem HD placenta (Figure 9). The increase in JZ area may be due to the increase of glycogen storage in the glycogen trophoblast cell. For the antagonist, Ex9, the JZ also has an increase in area but compared to the control it is not significant ($P=0.07$); however, there was a significant decrease in the LB zone cross sectional area ($P<0.009$) (Figure 8). Despite the increase in the JZ area in the Ex9 placenta, there was no difference in the PAS stain. Therefore, further investigation is needed to determine whether the increase in PAS stain is directly related to the increase in JZ area.

There was an overall increase in the male JZ area ratio between the treatments, but the only significant increase was between the control and Ex9 ($P<0.03$) (Figure 8). In the male LB zone, there is a decrease in the cross-sectional area ratio between Sem HD ($P<0.005$) and Ex9 ($P<0.002$) but not for the agonist low dosage ($P=0.3$) (Figure 8). In the male placenta DC area, there is an increase in the cross-sectional area between the control and agonist high dosage ($P<0.03$); however, the Sem was not significant ($P=0.38$) (Figure 8). The Ex9 treated male placenta was also not significant in the DC ($P=0.5$) (Figure 8). DC has been known to protect the fetus from maternal immune cells and provide nutritional support before the placenta is established (65); however, not much is known about the influence of the DC if there was an increase or decrease for the placenta. It is also important to note that parts of the decidua might have been cut to optimize the sectioning of the tissue. The placenta from female pups had an increase in JZ cross-sectional area ($p<0.03$) in Sem and a decrease in the LB cross-sectional area ($p<0.02$) (Figure 8). The Sem HD and Ex9 treated placentas from female pups did not show any significant difference in the three zones of placenta. Overall, the male and female placenta exhibit a decrease in the LB area and a slight increase in the JZ area.

Figure 8. Decrease in labyrinth (LB) zone areas in E18.5 placenta and increase in junctional (JZ) zone areas. Placental cross-sectional areas were determined by using Alkaline-Phosphatase (AP) stain placental sections. JZ, junctional zone; LB, labyrinth; DC, decidua. Cross-sectional area was calculated using ImageJ by dividing the different layers by the total area of the placenta. (a) Placenta area ratio of all the placenta that was harvested. Saline (N=21), Sem (N=20), Sem HD (N=16), Ex9 (N=11). There was a significant increase in the Sem JZ area ($P<0.006$) and decrease in Sem LB area ($P<0.003$). There is also a decrease in LB area in the Ex9 treatment ($P<0.009$). (b) Representative E18.5 placenta AP stain images. (c) Male placenta area ratio had a significant increase in JZ area ($P<0.03$) in Ex9 treatment and decrease in LB area ($P<0.002$). Sem HD treatment had a decrease in LB area ($P<0.005$) and increase in DC area ($P<0.03$). Saline (N=7), Sem (N=5), Sem HD (N=8), and Ex9 (N=5). (d) Female placenta area ratio had an increase in JZ area ($P<0.03$) and decrease in LB area ($P<0.02$). Saline (N=8), Sem (N=8), Sem HD (N=6), and Ex9 (N=6).

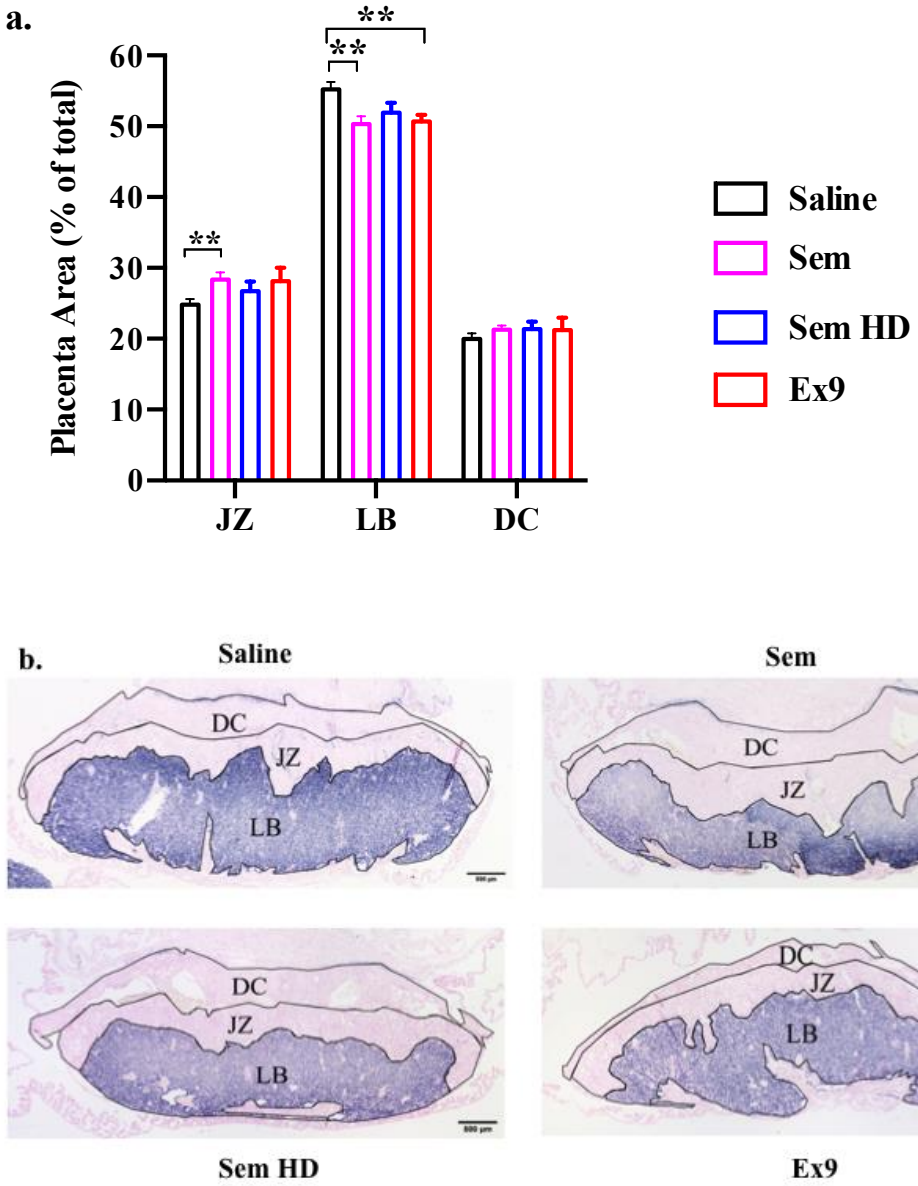
a.
Placenta Area (% of total)
60
50
40
30
20
10
0
**
**
**
JZ
LB
DC
Saline
Sem
Sem HD
Ex9
b.
Saline
Sem
DC
JZ
LB
Sem HD
Ex9
c.
Male Placenta Area (% of total)
*
**
**
*
d.
Female Placenta Area (% of total)
*
*

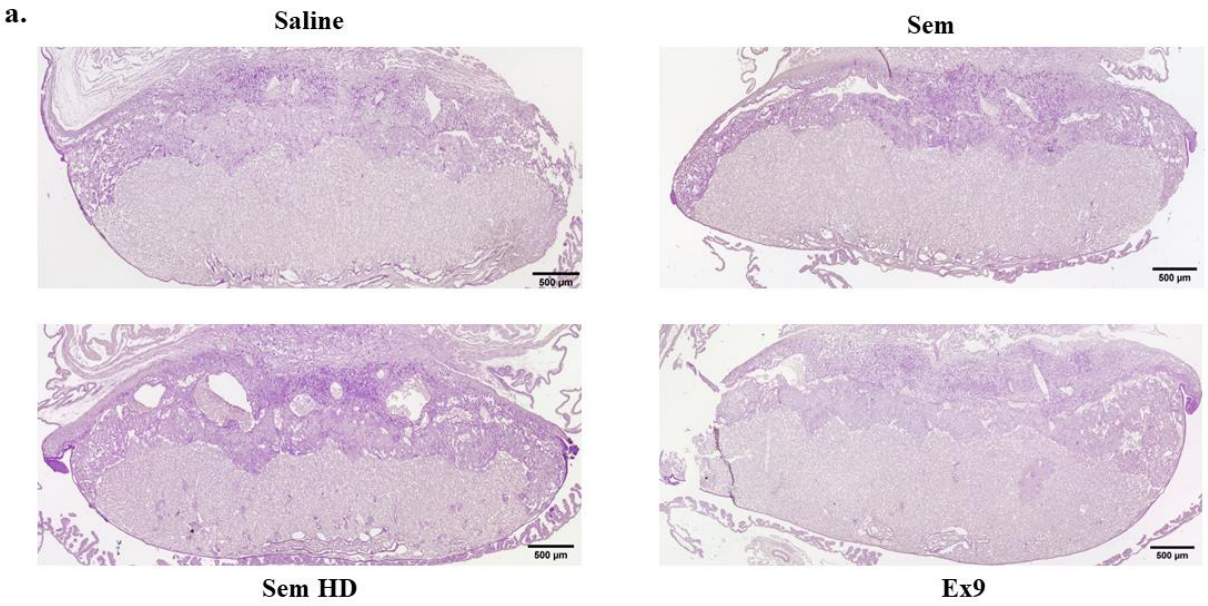

Figure 9. E18.5 PAS stain of Saline, Sem, Sem HD, and Ex9 placenta. PAS stain detects polysaccharides and mucosubstances. This includes glycogen, glycoproteins, glycolipids, and mucins in tissues. (a) There was an increase in the PAS staining in the junctional zone (jz) of the placenta in the Sem and Sem HD compared to saline. There was a visible slight decrease in the Ex9 placenta compared to saline.

The decrease in LB area reduced the transport area for nutrient exchange and restricts the potential growth the fetus will have. Furthermore, there were decreases in transporter protein mRNA levels, Snat1 and Glut1 in Sem low dosage injected dams ($p<0.008$ and $p<0.02$, respectively) also affects fetal growth (Figure 10). On the other hand, there is an increase in Lat1 and Snat2 transporter proteins in the Sem low dosage injected treatment ($P<0.01$ and $P<0.002$) (Figure 10). Additionally, there is also a decrease in the FABPdm mRNA levels ($P<0.011$) (Figure 10). The Sem HD transporter proteins had a decrease in SnatT1 mRNA levels ($P<0.003$) and a decrease although not significant in Lat1 mRNA, Glut1 mRNA, and FABPdm mRNA (Figure 10). With the reduction of some transporter proteins, it is plausible that the nutrient exchange rate between the dam and the fetus must have been affected by the injection; however, there were increases in other transporter proteins. Thus, the nutrient exchange via the protein transporters may not be the defining factor of the reduction of fetal weight.

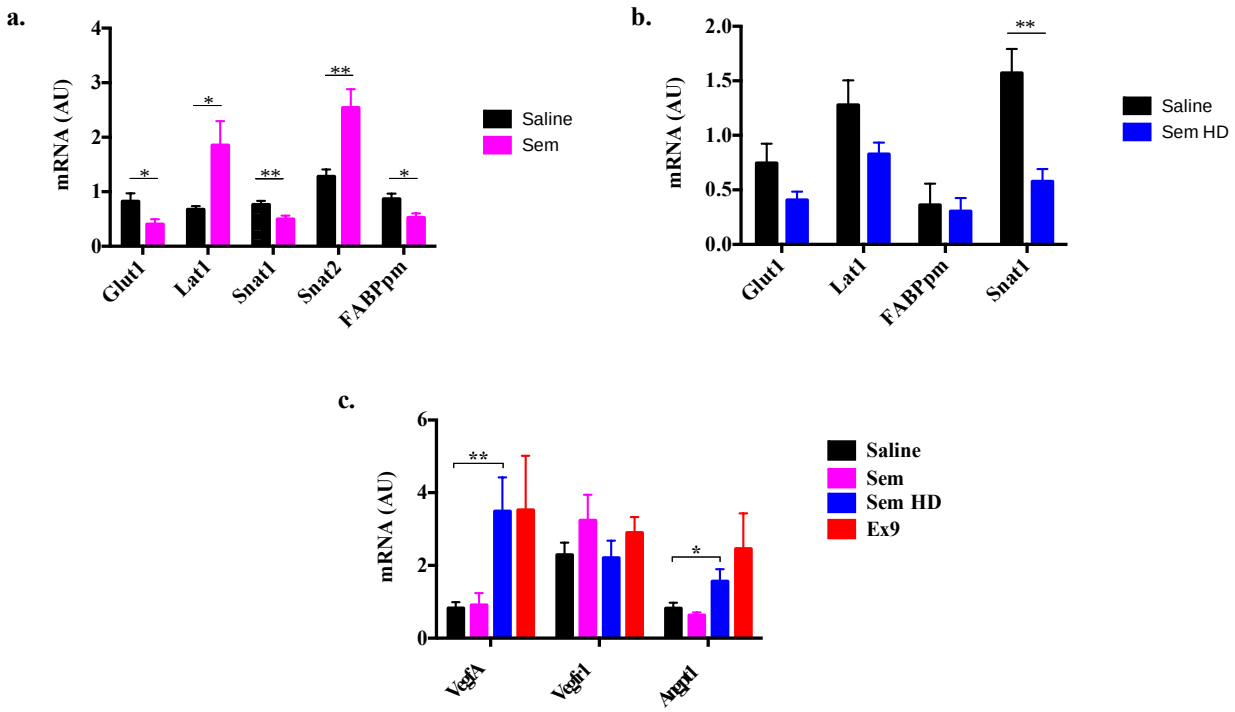

Figure 10. **mRNA levels of E18.5 placenta from Saline, Sem, Sem HD, and Ex9 treated dams**. All mRNA levels were normalized to 18S mRNA. (a) and (b) are mRNA levels of transporter proteins that had differences in Sem and Sem HD treatments. (c) is the mRNA levels of angiogenic factors that lead to or regulate angiogenesis.

The next step was to investigate the labyrinth zone, the area of nutrient exchange, to see if there are any significant differences in the vessels or factors that may affect fetal growth. Previous studies have shown that there are histological measurements to the vascularity of nutrient transferring tissues by calculating the capillary area, tissue area, the number of vessels, and the vascular surface area by immunohistochemistry (IHC) of platelet and endothelial cell adhesion molecule 1 (CD31) (66-68). CD31 is known as an endothelial cell marker that is expressed at the junctions between endothelial cells and is involved in angiogenesis by regulating endothelial cell migration (69-70). These measurements may explain the decrease in the LB area by vascular growth. The capillary area density (CAD) measures the blood flow, the capillary number density (CND) measures the vascular branching, the capillary surface density (CSD) measures the nutrient exchange, and the area per capillary (APC) measures the capillary size (68). There was a decrease in the CAD, CSD, and CND in the Sem low dosage treatment compared to the control ($P<0.005$ and $P<0.0006$, and $P<0.0006$, respectively) (Figure 11). The APC did not have a significant difference (Figure 11). This implies that the capillary size did not differ between the placentas, but the branching, nutrient exchange, and blood flow did have a decrease which matches the decrease in the LB zone. Thus, ultimately decreasing the potential growth of the fetus. Additionally, immunofluorescence (IF) intensity of CD31 was also calcualted by ImageJ by the ratio of CD31 fluorescence intensity and the labyrinth area. There was a decrease in fluorescence between Sem ($P<0.006$), Sem HD ($P<0.0003$), and Ex9 ($P<0.0003$) compared to saline (Figure 12). The most significant decrease was seen in the Sem HD and Ex9 placentas which coincide with the major reduction of fetal weight in those treated dams. In addition to the physical differences in the placenta vasculature, there is also the factors that can affect the placenta molecularly. There was an increase in Sem HD E18.5 placenta

mRNA levels of angiopoietin-1 (ANGPT1) ($P<0.05$), a stabilizing factor that regulates angiogenesis response, (Figure 10) (71) which attenuated angiogenesis within the placenta decreasing the chance of increasing surface area to exchange nutrients. There was also no significant difference in the VEGFR1 mRNA levels between the treatments; however, there was an increase in Vegfa mRNA levels of Sem HD placenta ($P<0.008$), known to play a critical role in angiogenesis and vasculogenesis, compared to saline mRNA levels (Figure 10) (72). Altogether, molecularly there is a contradiction within the angiogenic proteins and its influence on the placenta.

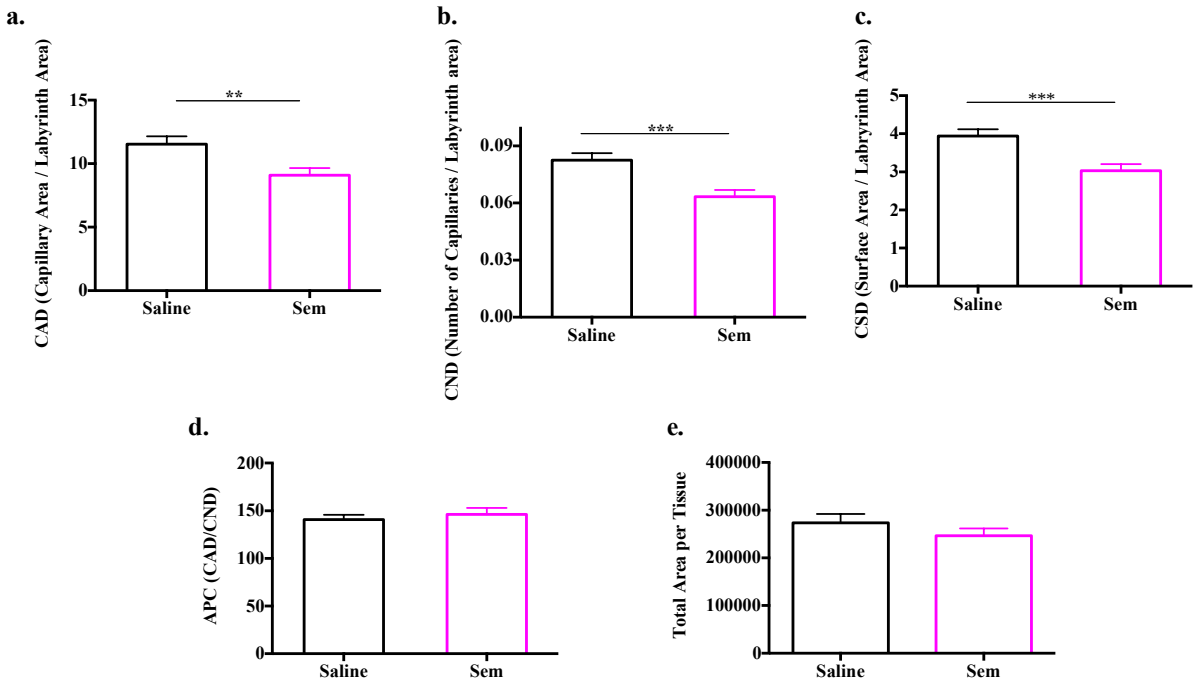

Figure 11. Immunohistochemistry of CD31 demonstrate a decrease in CAD, CND, CSD, APC within the E18.5 placenta. CAD, capillary area density. CND, capillary number density. CSD, capillary surface area density. APC, area per capillary. CAD is calculated by dividing the capillary area divided by the total area. CND is calculated by dividing the number of vessels by the total area. CSD is calcualted by dividing the perimeter of the capillaries to the total area. APC is calculated by dividing the area of CD31 and the number of vessels. All the measurements were made in ImageJ and calibrated to µm. (a) CAD per tissue area had a significant decrease in Sem placenta compared to saline ($P<0.005$). (b) CND per tissue area and (c) CSD per tissue area also had a reduction in Sem placenta ($P<0.0006$).

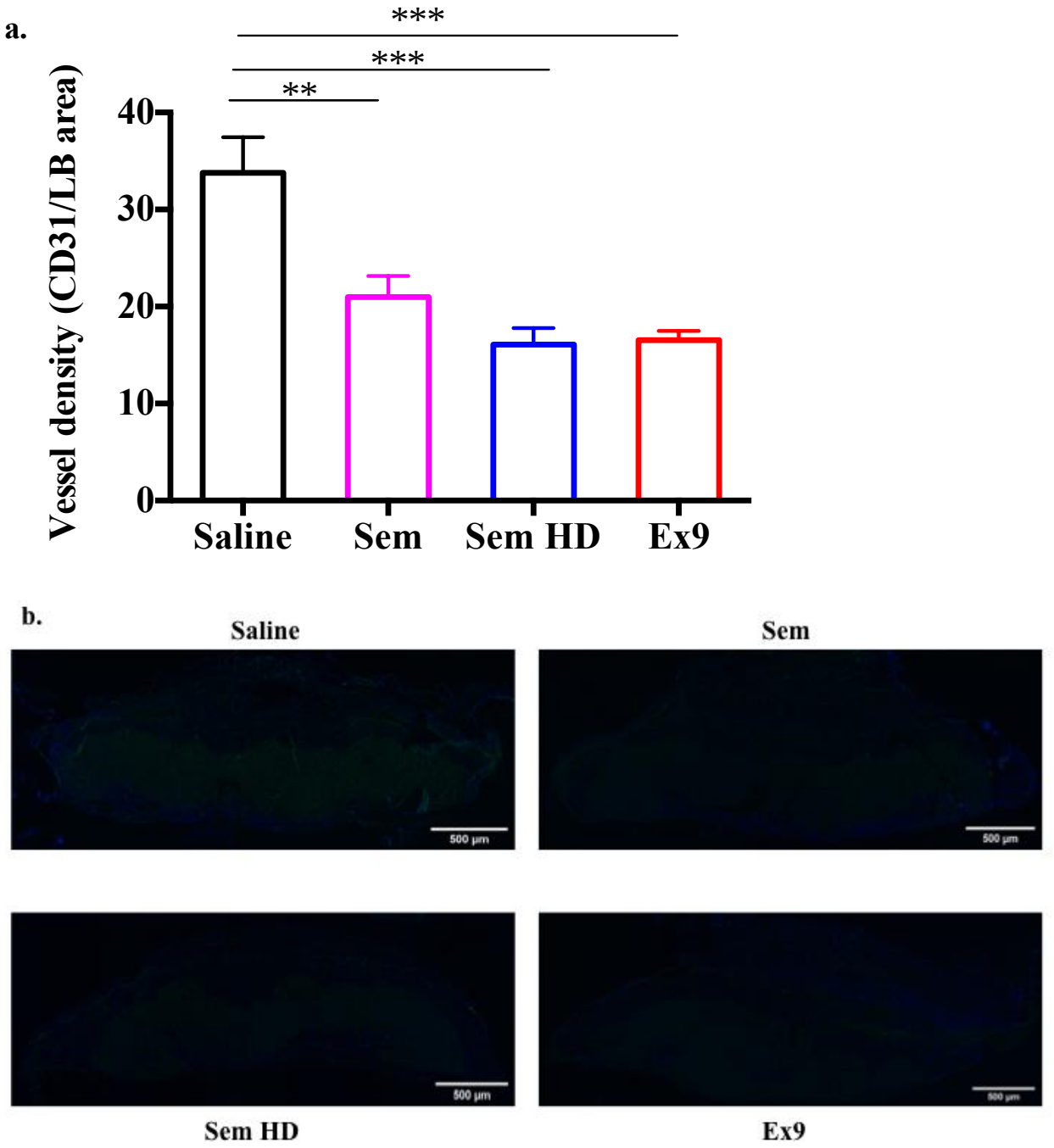

Figure 12. Immunofluorescence of CD31 signifies a reduction of vessel density within the Sem, Sem HD, and Ex9 placentas. Vessel density was calculated by the immunofluorescence intensity of CD31 by the labyrinth area. All the measurements were made in ImageJ and calibrated to µm. Saline (N=6), Sem (N=12), Sem HD (N=10), and Ex9 (N=8). (a) There was a significant decrease in the vessel density for Sem ($P<0.006$), Sem HD ($P<0.0003$), and Ex9 ($P<0.0003$). (b) Representative images for the various treatments.

DISCUSSION

Circulating GLP-1 has a major role in postprandial metabolism by potentiating nutrient-induced insulin secretion (73), inhibition of glucagon secretion (15), and reduction of gastric emptying (37-38). During pregnancy maternal metabolism changes substantially as sensitivity to insulin rises in dam's tissues leading to insulin resistance (58). Thus, GLP-1 may take part in maternal metabolism and fetal development. The injection of the agonist and antagonist of GLP-1R greatly changed the fetal development of the pups and had some affects that occurred in the dam. The dams had no significant difference in their body weight, fat, and lean fat composition from the EchoMRI that was done during pregnancy: E13.5, E15.5, and E18.5 for the Sem and Sem HD injected dams. The Ex9 injected dams did not have EchoMRI scans done. The fetal weight at E18.5 was decreased between the control and the treatments and no significant difference in the placenta weight (Figure 1). Previous studies have also demonstrated there was a decrease in the fetal weight and no difference in placenta weight from dams that were injected with GLP-1R agonist and antagonist (74-76). The placenta efficiency ratio, dividing the pups' weight with the placenta weight, was also not significant for the GLP-1R agonist treatments but was significant for the antagonist treatment (Figure 2). Indicating that the reduction of fetal weight in the antagonist treatment was due to the placenta. Since pregnancy changes the dynamics of metabolism within the dam's body to optimize the transfer of nutrients to the fetus, the maternal metabolism of the treatments during late pregnancy needs to be investigated.

The E18.5 dam glucose and insulin serum levels had no difference between the treatments (Figure 3); however, there was an observed transient change in Sem treated and Ex9 treated dams in glucose and insulin serum levels (Figure 4). The observed transient decrease in glucose levels most likely caused the decrease in the fetal weight in the Sem treated dams

(Figure 4) while the Ex9 treated dams had a decrease in pup's weight due to the inefficiency of the placenta (Figure 2) to transfer nutrients to the fetus as the increase of glucose levels after the Ex9 injection in the E15.5 fed serum levels displayed there is an ample amount of glucose available to transfer to the fetus but there must be issues with the transfer of the nutrients which caused the decrease. It must be noted that with the E15.5 serum levels after injection that the dams recovered from the treatment injections regardless of treatment. For the Sem high dosage treatment injection the glucose levels recovered after an 8-hour period while the insulin levels recovered in 2-hours (Figure 4). The Ex9 treatment recovered glucose levels after the increase in four hours and the insulin levels within an hour (Figure 4). The next injection for the treatments were then done within 48 hours of the previous injection, giving the dams even more time to adapt or recover to the previous conditons. Therefore, the E18.5 serum levels for glucose and insulin did not have any significant difference, but the injections did influence the dams as there is an increase in the β – cell area ratio for the Sem high dosage treatment while the Ex9 treatment had a slight decrease. Furthermore, there was a decrease of the α – cell ratio area of the dam's islets in all the treatments, but only significantly decreased in the Ex9 treatment (Figure 5). As GLP-1R is known to promote β – cell expansion it makes sense that there is an increase of the ratio to the pancreas; however, the effect that was shown in the α-cell ratio was unpreceded as it is unknown if there would be such an effect on the α-cell (33).

Notably, there is a decrease in E18.5 fetal insulin serum levels and a decrease in the E18.5 pups glucose serum levels in the Sem high dosage and Ex9 compared to the saline (control) group. Insulin deficiency in the fetus can cause the decrease in fetal growth or development and with the decrease in glucose levels there is a reduced energy supply for the pups to grow (59,60). The fetal insulin deficiency may be due to the deficiency in nutrients, the

production of insulin in the β – cell, or reduced sensitivity to insulin in tissues by their receptors (59); however, the β – cell area ratio for the E18.5 fetal pancreas had no significant difference between the control and the agonist or antagonist (Figure 5). As there is no difference in the β – cell area ratio of the pancreas, there must be no difference in the insulin secretion within the β – cell. The brief reduction of glucose after the injection of the agonist could be the cause of the fetal insulin serum level reduction; however, there was no observed transient decline in the antagonist injected glucose serum levels. Thus, there must be a sensitivity to insulin within other tissues. Moreover, the pups' skeletal muscle and liver western blots indicate that there is an increase in p-GSK3 by the band intensity which is known to induce insulin resistance by the phosphorylation of insulin receptor substrate – 1 (IRS1) (61) (Figure 6). Noting that the increase in p-GSK3 is seen in the agonist (Sem) treated fetal tissue and there is no data for the antagonist (Exendin=9) fetal tissue. Interestingly, the α – cell area ratio for the E18.5 pups had significant decrease in all the treatments compared to the control. This reduction of the α – cell ratio could indicate that the GLP-1R agonist and antagonist can pass through the placenta and affect the pups by reducing glucagon secretion from the α – cells; however, since there is no increase in insulin secretion further investigation is needed to determine whether it is due to the agonist or antagonist that passed through the placenta. The agonist that was used, Semaglutide, is known to pass through the placenta of rats (56) and most likely could pass through the placenta of the mice. For the antagonist, Avexitide, further investigation is needed to determine this.

Growth factors from maternal or fetal origin will affect fetal and placenta growth. The most prominent is the IGF system which comprises of two ligands, insulin-like growth factor-1 (IGF-1) and insulin-like growth factor-2 (IGF-2), and the six insulin-like growth factor binding proteins (IGFBPs) with the two receptors, insulin-like growth factor receptor 1 (IGFR1) and

insulin-like growth factor receptor 2 (IGFR2) (77). IGF-2 is the primary growth factor for embryonic growth and IGF-1 during gestation (77). Interestingly, there was an increase in the Sem low dosage IGF-1 levels in the fetal serum while there was no significant difference in the Sem high dosage and the Ex9 fetal serum (Figure 7). Additionally, there was a decrease trend in the western blot E18.5 IGFBP-1 serum band densities for both Sem high dosage and Ex9 (Figure 7). With less IGFBP-1, it is possible that there is less IGF-1 in the serum as the IGFBP-1 has a higher affinity of IGF-1 than its receptor IGFR (78). However, further investigation is needed to confirm this and exemplify the reason behind the increase of the IGF-1 serum in Sem low dosage levels.

Furthermore, the overall decrease in LB area and increase in JZ area indicated the physical difference of the placenta between the treatments (Figure 8). The decrease in the LB area as stated earlier, reduced the area of exchange of nutrients between the dam and the fetus. Although there is an observed decrease in LB area, the transporter proteins had conflicting results as there were some transporter proteins that had a decrease in mRNA levels and others with an increase (Figure 10). Thus, it is difficult to conclude that it is due to the decrease of available transporter protein in the placenta to cause the decrease in the fetal weight. Additionally, the overall increase in the JZ area coincide with the increase PAS-stained placenta in the Sem treated placentas compared to saline (Figure 9). Previous studies led to the hypothesis that placental glycogen provide a source of glucose to support fetal growth during late gestation; however, how placental glycogen is metabolized is still not well understood (64). Typically, the JZ area will expand until it reaches E16.5 and then reduce by E18.5 indicating that the glycogen might be utilized during the rapid fetal growth period during late gestation (64,79). If this is true, then the glycogen that was stored in the Sem treated placentas was not utilized during the rapid

fetal growth period resulting in the increase of PAS-stained placenta JZ. Although it is plausible, the Ex9 treated placenta did not showcase an increase in intensity of the PAS-stained placenta; thus, the utilization of the glycogen may not be the reason behind the reduction of the Ex9 fetal weight. Interestingly, the cross-sectional area for the different layers of the placenta did not exhibit a difference between sex (Figure 8). There's an overall observed decrease in the LB area and an increase in the JZ area for both male and female (Figure 8). This coincides with the fetal weight decrease which is observed in both male and female where there are significant decreases in some treatments versus others that do decrease but are not significant.

As mentioned previously, the malfunction of the placenta, leads to IUGR which is the restriction or limitation of growth for the fetus (80). Hence, placenta development is important to note as the placenta plays a support role for the growth of the fetus. Previous studies have used vascular development and angiogenic factors to understand the developing placenta by calculating vascular growth (59,63,81). Vascular growth can be calcualted by determining the capillary area density, number of capillaries, surface area density, and area per capillary within the labyrinth area. The initial implantation of the placenta is important in establishing the first blood vessels that ensure the transfer of nutrients to the fetus (82). This process is mainly vascuologenesis, the formation of the first blood vessels by differentiation of mesenchymal cells into haemangiogenic stem cells (82). After that most of the vessels that arise from the placenta are from angiogenesis, the formation of blood vessels from existing blood vessels (82,83). With the reduction of CAD, CND, and CSD in the Sem placenta compared to the control, the placenta exhibits a decrease in blood flow, vascular branching, and nutrient exchange (Figure 11). This reduction leads to the decrease in the fetal weight in addition to the decreased levels of fetal insulin and glucose. Furthermore, there was a decrease in vessel density within the agonist and

antagonist placenta compared to saline (Figure 12). The vessel density was calculated by the fluorescence intensity of CD31 on the placenta. The decrease in vessel density further demonstrated the decrease of angiogenesis within the placenta. Previous studies have found that there are GLP-1Rs in the endothelium, cardiac myocytes, and vascular myocytes in mice (84,85). Moreover, there was co-expression of the GLP-1R in the smooth muscle actin in mice ventricular blood vessels (24,84). However, there were also studies that failed to identify GLP1-R mRNA transcripts within the coronary artery smooth muscle actins in humans (86). GLP-1R expression remains conclusively determined whether the GLP-1R is expressed in the vascular endothelium of animals or humans and if it is specific to vascular beds which include the placenta vessels (85). Despite this, there are studies that showcase intravenous infusion of native GLP-1 that demonstrated significant improvements in rat microvascular blood volume and microvascular blood flow (87). Additionally, in previous studies GLP-1R agonists promoted angiogenesis in endothelial cells by upregulating the tissue expression of angiogenic factors such as endothelial NOS (eNOS), VEGF, and basic fibroblast growth factor (bFGF) (88,88,90). Cultured studies of GLP-1 treatment to endothelial progenitor cells also demonstrated an increase in VEGF levels promoting proliferation, migration, and maturation of endothelial cells (91). Indicating that there is a direct effect of GLP-1 on endothelial cells by VEGF. Moreover, in a previous study GLP-1Rs in endothelial cells had reduced VEGFA-mediated vasodilation by the GLP-1 activation of the G_s – coupled pathway which interact with the Src kinase that is known to control signaling pathways that lead to the control of vessel tone (72). This leads to the delayed release of Ca^{2+} which is needed for the activation of vasodilation via eNOS (71). Interestingly, there was an increase in VEGFA mRNA levels within the E18.5 placenta in the Sem HD and slight increase in Ex9 placentas (Figure 9). The increase in VEGFA mRNA levels

indicate the compensation or homeostasis response of the delay to promote the angiogenesis and vasodilation of endometrial endothelium cells (92,93). In addition to this, there was also an increase in ANGPT1 mRNA levels in Sem HD and Ex9 placentas (Figure 9) to compensate for the delay by regulating angiogenesis (71). In Sem HD, there was an overexpression of GLP-1 by the agonist binding to GLP-1Rs which most likely caused the increase of production of ANGPT1 in the placenta to regulate angiogenesis by decreasing the amount of branching or new vessels being made. This is not seen in the Sem (low dosage) treatment as the amount of GLP-1R injected was not enough to affect the placenta. Thus, other factors may be the cause of the decrease in angiogenesis; however, the overexpression or the blockage of the GLP-1R within the placenta additionally could cause the decrease in the fetal weight. In Ex9 placentas, the antagonist completely blocks out the pathway in which GLP-1R promotes angiogenesis and vasodilation which eventually affects the placenta. This can be seen by the decrease of placenta efficiency ratio of the Ex9 injected dams. Further investigation within the angiogenesis pathway of the placenta and its development is needed to figure out the reduction of fetal weight.

Overall, the decline in fetal weight due to the GLP-1R agonist injections during late pregnancy was ascribed by the transient decrease of glucose serum levels in the dam which led to the reduction of glucose availability to transfer to the fetus. Hormones such as insulin and IGF-1 play a major role in fetal development; however, with varying contradictions in the fetal IGF-1 serum levels it is difficult to determine whether it is the cause of the reduction and the fetal insulin deficiency from the insulin resistance in fetal tissue needs further investigation as there is no data for the antagonist western blot of fetal tissue. In addition to the reduction, there was also diminished angiogenesis occuring in the placenta that will further reduce the surface area availble to transfer nutrients. This can be depicted in the diminished labyrinth zone where the

exchange takes place. Whether there is a direct affect or not is still debated, however, there may be an indirect affect from the agonist injection. On the other hand, the GLP-1R antagonist injections also had a decline in fetal weight due to the deficiency of the placenta in transferring nutrients to the fetus which include the reduction of labyrinth zone area and the blockage of GLP-1R induced angiogenesis. Interestingly, the GLP-1R agonist and antagonist had the same results for the reduced fetal weight, fetal glucose and insulin serum levels, and the reduction of vessel density. It is worth noting that the GLP-1R antagonist had a small sample size compared to the agonist injected dams; thus, further studies are needed to determine whether this result is the cause of the injection. Further investigation is also needed to determine GLP-1R in the endothelium of the placenta capillaries whether the angiogenesis reduction was directly due to the GLP-1 agonist or antagonist.

ACKNOWLEDGEMENTS

This thesis is currently being prepared for submission for publication. The thesis author was the primary author of this paper with Liping Qiao and Jianhua Shao as co-authors.

REFERENCES

1. McLean Brent A, Wong Chi Kin, Campbell Jonathan E, Hodson David J, Trapp Stefan, Drucker Daniel J, Revisiting the Complexity of GLP-1 Action from Sites of Synthesis to Receptor Activation, *Endocrine Reviews*, Volume 42, Issue 2, April 2021, Pages 101–132, https://doi.org/10.1210/endrev/bnaa032.

2. Bell GI, Sanchez-Pescador R, Laybourn PJ, Najarian RC. Exon duplication and divergence in the human preproglucagon gene. *Nature*. 1983;304(5924):368-371.

3. Campbell JE, Drucker DJ. Pharmacology, physiology, and mechanisms of incretin hormone action. *Cell Metabolism*. 2013 Jun 4;17(6):819-837. doi: 10.1016/j.cmet.2013.04.008. Epub 2013 May 16. PMID: 23684623.

4. Unger R.H., Eisentraut A.M., Mc C.M., Keller S., Lanz H.C., Madison L.L. Glucagon antibodies and their use for immunoassay for glucagon. *Proceedings of The Society for Experimental Biology and Medicine.* 1959; 102:621–623

5. Samols E., Marks V. New conceptions on the functional significance of glucagon (pancreatic and extra-pancreatic) *Journees Annuelles de Diabetologie de l'Hotel-Dieu.* 1967; 7:43–66.

6. Unger R.H., Ohneda A., Valverde I., Eisentraut A.M., Exton J. Characterization of the responses of circulating glucagon-like immunoreactivity to intraduodenal and intravenous administration of glucose. *Journal of Clinical Investigation.* 1968; 47:48–65.

7. Maigen Bethea, Nadejda Bozadjieva-Kramer, Darleen A Sandoval, Preproglucagon Products and Their Respective Roles Regulating Insulin Secretion, *Endocrinology*, Volume 162, Issue 10, October 2021, bqab150, https://doi.org/10.1210/endocr/bqab150

8. Trapp S, Cork SC. PPG neurons of the lower brain stem and their role in brain GLP-1 receptor activation. *Am J Physiol Regul Integr Comp Physiol*. 2015 Oct 15;309(8): R795-804. doi: 10.1152/ajpregu.00333.2015. Epub 2015 Aug 19. PMID: 26290108; PMCID: PMC4666945.

9. Rouillé Y, Martin S, Steiner DF. Differential processing of proglucagon by the subtilisin-like prohormone convertases PC2 and PC3 to generate either glucagon or glucagon-like peptide. *J Biol Chem*. 1995 Nov 3;270(44):26488-96. doi: 10.1074/jbc.270.44.26488. PMID: 7592866.

10. Mojsov S, Heinrich G, Wilson IB, Ravazzola M, Orci L, Habener JF. Preproglucagon gene expression in pancreas and intestine diversifies at the level of post-translational processing. *J Biol Chem*. 1986 Sep 5;261(25):11880-9. PMID: 3528148.

11. Nie Y, Nakashima M, Brubaker PL, Li QL, Perfetti R, Jansen E, Zambre Y, Pipeleers D, Friedman TC. Regulation of pancreatic PC1 and PC2 associated with increased glucagon-like peptide 1 in diabetic rats. *J Clin Invest*. 2000 Apr;105(7):955-65. doi: 10.1172/JCI7456. PMID: 10749575; PMCID: PMC377475.

12. Dhanvantari S, Seidah NG, Brubaker PL. Role of prohormone convertases in the tissue-specific processing of proglucagon. *Mol Endocrinol*. 1996 Apr;10(4):342-55. doi: 10.1210/mend.10.4.8721980. PMID: 8721980.

13. Rothenberg ME, Eilertson CD, Klein K, Zhou Y, Lindberg I, McDonald JK, Mackin RB, Noe BD. Processing of mouse proglucagon by recombinant prohormone convertase 1 and immunopurified prohormone convertase 2 in vitro. *J Biol Chem*. 1995 Apr 28;270(17):10136-46. doi: 10.1074/jbc.270.17.10136. PMID: 7730317.

14. Nadkarni P, Chepurny OG, Holz GG. Regulation of glucose homeostasis by GLP-1. *Prog Mol Biol Transl Sci*. 2014;121:23-65. doi: 10.1016/B978-0-12-800101-1.00002-8. PMID: 24373234; PMCID: PMC4159612

15. Ramracheya R, Chapman C, Chibalina M, Dou H, Miranda C, González A, Moritoh Y, Shigeto M, Zhang Q, Braun M, Clark A, Johnson PR, Rorsman P, Briant LJB. GLP-1 suppresses glucagon secretion in human pancreatic alpha-cells by inhibition of P/Q-type Ca^{2+} channels. *Physiol Rep*. 2018 Sep;6(17):e13852. doi: 10.14814/phy2.13852. PMID: 30187652; PMCID: PMC6125244.

16. Drucker, Daniel J. "The Biology of Incretin Hormones," Cell Metabolism, Cell Press, 7 Mar. 2006, https://www.sciencedirect.com/science/article/pii/S1550413106000283.

17. Baggio LL, Drucker DJ. Biology of incretins: GLP-1 and GIP. *Gastroenterology*. 2007 May;132(6):2131-57. doi: 10.1053/j.gastro.2007.03.054. PMID: 17498508.

18. MacDonald PE, El-Kholy W, Riedel MJ, Salapatek AM, Light PE, Wheeler MB. The multiple actions of GLP-1 on the process of glucose-stimulated insulin secretion. *Diabetes*. 2002 Dec;51 Suppl 3:S434-42. doi: 10.2337/diabetes.51.2007.s434. PMID: 12475787.

19. Holst JJ. The physiology of glucagon-like peptide 1. *Physiol* Rev. 2007 Oct;87(4):1409-39. doi: 10.1152/physrev.00034.2006. PMID: 17928588.

20. Ghosal, Sriparna, Myers, Brent, Herman, James P., "Role of Central Glucagon-like Petpide-1 in Stress Regulation." *Physiology & Behavior*, Elsevier, 24 Apr.2013.https://doi.org/10/1016/j.physbeh.2013.04.003

21. Burcelin R. The gut-brain axis: a major glucoregulatory player. *Diabetes Metab*. 2010 Oct;36 Suppl 3:S54-8. doi: 10.1016/S1262-3636(10)70468-7. PMID: 21211737.

22. Shigeto M, Katsura M, Matsuda M, Ohkuma S, Kaku K. Low, but physiological, concentration of GLP-1 stimulates insulin secretion independent of the cAMP-dependent protein kinase pathway. *J Pharmacol Sci*. 2008 Nov;108(3):274-9. doi: 10.1254/jphs.08090fp. Epub 2008 Nov 6. PMID: 18987435.

23. Abu-Hamdah R, Rabiee A, Meneilly GS, Shannon RP, Andersen DK, Elahi D. Clinical review: The extrapancreatic effects of glucagon-like peptide-1 and related peptides. *J Clin Endocrinol Metab*. 2009 Jun;94(6):1843-52. doi: 10.1210/jc.2008-1296. Epub 2009 Mar 31. PMID: 19336511; PMCID: PMC2690432.

24. Richards P, Parker HE, Adriaenssens AE, Hodgson JM, Cork SC, Trapp S, Gribble FM, Reimann F. Identification and characterization of GLP-1 receptor-expressing cells using a new transgenic mouse model. Diabetes. 2014 Apr;63(4):1224-33. doi: 10.2337/db13-1440. Epub 2013 Dec 2. PMID: 24296712; PMCID: PMC4092212.

25. Farkas E, Szilvásy-Szabó A, Ruska Y, Sinkó R, Rasch MG, Egebjerg T, Pyke C, Gereben B, Knudsen LB, Fekete C. Distribution and ultrastructural localization of the glucagon-like peptide-1 receptor (GLP-1R) in the rat brain. Brain Struct Funct. 2021 Jan;226(1):225-245. doi: 10.1007/s00429-020-02189-1. Epub 2020 Dec 20. PMID: 33341919; PMCID: PMC7817608.

26. Drucker DJ. Mechanisms of Action and Therapeutic Application of Glucagon-like Peptide-1. *Cell Metab*. 2018 Apr 3;27(4):740-756. doi: 10.1016/j.cmet.2018.03.001. PMID: 29617641.

27. Mayo KE, Miller LJ, Bataille D, Dalle S, Göke B, Thorens B, Drucker DJ. International Union of Pharmacology. XXXV. The glucagon receptor family. *Pharmacol Rev*. 2003 Mar;55(1):167-94. doi: 10.1124/pr.55.1.6. PMID: 12615957.

28. Underwood CR, Garibay P, Knudsen LB, Hastrup S, Peters GH, Rudolph R, Reedtz-Runge S. Crystal structure of glucagon-like peptide-1 in complex with the extracellular domain of the glucagon-like peptide-1 receptor. *J Biol Chem*. 2010 Jan 1;285(1):723-30. doi: 10.1074/jbc.M109.033829. Epub 2009 Oct 27. PMID: 19861722; PMCID: PMC2804221.

29. Drucker DJ, Philippe J, Mojsov S, Chick WL, Habener JF. Glucagon-like peptide I stimulates insulin gene expression and increases cyclic AMP levels in a rat islet cell line.

Proc Natl Acad Sci U S A. 1987 May;84(10):3434-8. doi: 10.1073/pnas.84.10.3434. PMID: 3033647; PMCID: PMC304885.

30. Koole, Cassandra, Pabreja, Kavita, Savage, Emelia E., Wootten, Denise, Furness, Sebastian G.B., Miller, Laurence J., Christopoulos, Arthur, Sexton, Patrick M.; Recent advances in understanding GLP-1R (glucagon-like peptide-1 receptor) function. *Biochem Soc Trans* 1 February 2013; 41 (1): 172–179. doi: https://doi.org/10.1042/BST20120236

31. Hällbrink M, Holmqvist T, Olsson M, Ostenson CG, Efendic S, Langel U. Different domains in the third intracellular loop of the GLP-1 receptor are responsible for Galpha(s) and Galpha(i)/Galpha(o) activation. *Biochim Biophys Acta*. 2001 Mar 9;1546(1):79-86. doi: 10.1016/s0167-4838(00)00270-3. PMID: 11257510.

32. Holz GG. Epac: A new cAMP-binding protein in support of glucagon-like peptide-1 receptor-mediated signal transduction in the pancreatic beta-cell. *Diabetes*. 2004 Jan;53(1):5-13. doi: 10.2337/diabetes.53.1.5. PMID: 14693691; PMCID: PMC3012130

33. Müller TD, Finan B, Bloom SR, D'Alessio D, Drucker DJ, Flatt PR, Fritsche A, Gribble F, Grill HJ, Habener JF, Holst JJ, Langhans W, Meier JJ, Nauck MA, Perez-Tilve D, Pocai A, Reimann F, Sandoval DA, Schwartz TW, Seeley RJ, Stemmer K, Tang-Christensen M, Woods SC, DiMarchi RD, Tschöp MH. Glucagon-like peptide 1 (GLP-1). *Mol Metab*. 2019 Dec; 30:72-130. doi: 10.1016/j.molmet.2019.09.010. Epub 2019 Sep 30. PMID: 31767182; PMCID: PMC6812410.

34. Buteau J, Roduit R, Susini S, Prentki M. Glucagon-like peptide-1 promotes DNA synthesis, activates phosphatidylinositol 3-kinase and increases transcription factor pancreatic and duodenal homeobox gene 1 (PDX-1) DNA binding activity in beta (INS-1)-cells. *Diabetologia*. 1999 Jul;42(7):856-64. doi: 10.1007/s001250051238. PMID: 10440129.

35. Zhu X, Oguh A, Gingerich MA, Soleimanpour SA, Stoffers DA, Gannon M. Cell Cycle Regulation of the Pdx1 Transcription Factor in Developing Pancreas and Insulin-Producing β-Cells. *Diabetes*. 2021 Apr;70(4):903-916. doi: 10.2337/db20-0599. Epub 2021 Feb 1. PMID: 33526589; PMCID: PMC7980191.

36. Wilcox G. Insulin and insulin resistance. *Clin Biochem Rev*. 2005 May;26(2):19-39. PMID: 16278749; PMCID: PMC1204764.

37. Maselli DB, Camilleri M. Effects of GLP-1 and Its Analogs on Gastric Physiology in Diabetes Mellitus and Obesity. *Adv Exp Med Biol*. 2021;1307:171-192. doi: 10.1007/5584_2020_496. PMID: 32077010.

38. Dailey MJ, Moran TH. Glucagon-like peptide 1 and appetite. *Trends Endocrinol Metab*. 2013 Feb;24(2):85-91. doi: 10.1016/j.tem.2012.11.008. Epub 2013 Jan 16. PMID: 23332584; PMCID: PMC3594872.

39. Wang Y, Egan JM, Raygada M, Nadiv O, Roth J, Montrose-Rafizadeh C. Glucagon-like peptide-1 affects gene transcription and messenger ribonucleic acid stability of components of the insulin secretory system in RIN 1046-38 cells. *Endocrinology*. 1995 Nov;136(11):4910-7. doi: 10.1210/endo.136.11.7588224. PMID: 7588224.

40. Asplund K, Westman S, Hellerström C. Glucose stimulation of insulin secretion from the isolated pancreas of foetal and newborn rats. *Diabetologia*. 1969 Aug;5(4):260-2. doi: 10.1007/BF01212095. PMID: 4902721.

41. Espinosa de los Monteros, Driscoll SG, Steinke J. Insulin release from isolated human fetal pancreatic islets. *Science*. 1970 May 29;168(3935):1111-2. doi: 10.1126/science.168.3935.1111. PMID: 4909765.

42. Lain KY, Catalano PM. Metabolic changes in pregnancy. *Clin Obstet Gynecol*. 2007 Dec;50(4):938-48. doi: 10.1097/GRF.0b013e31815a5494. PMID: 17982337.

43. Nolan CJ, Proietto J. The feto-placental glucose steal phenomenon is a major cause of maternal metabolic adaptation during late pregnancy in the rat. *Diabetologia*. 1994 Oct;37(10):976-84. doi: 10.1007/BF00400460. PMID: 7851692.

44. Baeyens L, Hindi S, Sorenson RL, German MS. β-Cell adaptation in pregnancy. *Diabetes Obes Metab*. 2016 Sep;18 Suppl 1(Suppl 1):63-70. doi: 10.1111/dom.12716. PMID: 27615133; PMCID: PMC5384851.

45. Moyce BL, Dolinsky VW. Maternal β-Cell Adaptations in Pregnancy and Placental Signalling: Implications for Gestational Diabetes. *Int J Mol Sci*. 2018 Nov 5;19(11):3467. doi: 10.3390/ijms19113467. PMID: 30400566; PMCID: PMC6274918.

46. Catalano PM, Tyzbir ED, Roman NM, Amini SB, Sims EA. Longitudinal changes in insulin release and insulin resistance in nonobese pregnant women. *Am J Obstet Glynecol*. 1991 Dec;165(6 Pt 1):1667-72. Doi:10.1016/0002-9378(91)90012-g. PMID: 1750458.

47. Qiao L, Shetty SK, Spitler KM, Wattez JS, Davies BSJ, Shao J. Obesity Reduces Maternal Blood Triglyceride Concentrations by Reducing Angiopoietin-Like Protein 4 Expression in Mice. *Diabetes*. 2020 Jun;69(6):1100-1109. doi: 10.2337/db19-1181. Epub 2020 Feb 12. PMID: 32051149; PMCID: PMC7243287.

48. Qiao L, Wattez JS, Lee S, Nguyen A, Schaack J, Hay WW Jr, Shao J. Adiponectin Deficiency Impairs Maternal Metabolic Adaptation to Pregnancy in Mice. *Diabetes*. 2017 May;66(5):1126-1135. doi: 10.2337/db16-1096. Epub 2017 Jan 10. PMID: 28073830; PMCID: PMC5399613.

49. Butte NF. Carbohydrate and lipid metabolism in pregnancy: normal compared with gestational diabetes mellitus. *Am J Clin Nutr*. 2000 May;71(5 Suppl):1256S-61S. doi: 10.1093/ajcn/71.5.1256s. PMID: 10799399.

50. Angueira AR, Ludvik AE, Reddy TE, Wicksteed B, Lowe WL Jr, Layden BT. New insights into gestational glucose metabolism: lessons learned from 21st century approaches. *Diabetes*. 2015 Feb;64(2):327-34. doi: 10.2337/db14-0877. PMID: 25614666; PMCID: PMC4876793.

51. Moffett, R. Charlotte, Vasu, Srividya, Thorens, Bernard, Drucker, Daniel J., Flatt, Peter R. Incretin Receptor Null Mice Reveal Key Role of GLP-1 but Not GIP in Pancreatic Beta Cell Adaptation to Pregnancy. *PLoS ONE*. 13 Jun. 2014. https://doi.org/10.1371/journal.pone.0096863.

52. Nikolic D, Al-Rasadi K, Al Busaidi N, Al-Waili K, Banerjee Y, Al-Hashmi K, Montalto G, Rizvi AA, Rizzo M, Al-Dughaishi T. Incretins, Pregnancy, and Gestational Diabetes. *Curr Pharm Biotechnol*. 2016;17(7):597-602. doi: 10.2174/1389201017666160127110125. PMID: 26813306.

53. Pereira de Arruda EH, Vieira da Silva GL, da Rosa-Santos CA, Arantes VC, de Barros Reis MA, Colodel EM, Gaspar de Moura E, Lisboa PC, Carneiro EM, Damazo AS, Latorraca MQ. Protein restriction during pregnancy impairs intra-islet GLP-1 and the expansion of β-cell mass. *Mol Cell Endocrinol.* 2020 Dec 1;518:110977. doi: 10.1016/j.mce.2020.110977. Epub 2020 Aug 11. PMID: 32791189.

54. Sukumar N, Bagias C, Goljan I, Weldeselassie Y, Gharanei S, Tan BK, Holst JJ, Saravanan P. Reduced GLP-1 Secretion at 30 Minutes After a 75-g Oral Glucose Load Is Observed in Gestational Diabetes Mellitus: A Prospective Cohort Study. *Diabetes*. 2018 Dec;67(12):2650-2656. doi: 10.2337/db18-0254. Epub 2018 Sep 19. PMID: 30232211.

55. Bonde L, Vilsbøll T, Nielsen T, Bagger JI, Svare JA, Holst JJ, Larsen S, Knop FK. Reduced postprandial GLP-1 responses in women with gestational diabetes mellitus. *Diabetes Obes Metab*. 2013 Aug;15(8):713-20. doi: 10.1111/dom.12082. Epub 2013 Mar 12. PMID: 23406269.

56. European Medicines Agency: EMA/CHMP/715701/2017 – Assessment report of Ozempic, https://www.ema.europa.eu/en/documents/assessment-report/ozempic-epar-public-assessment-report_en.pdf, August 2022.

57. Graham DL, Madkour HS, Noble BL, Schatschneider C, Stanwood GD. Long-term functional alterations following prenatal GLP-1R activation. *Neurotoxicol Teratol*. 2021 Sep-Oct;87:106984. doi: 10.1016/j.ntt.2021.106984. Epub 2021 Apr 20. PMID: 33864929; PMCID: PMC8555578.

58. Sonagra AD, Biradar SM, K D, Murthy D S J. Normal pregnancy- a state of insulin resistance. *J Clin Diagn Res*. 2014 Nov;8(11):CC01-3. doi: 10.7860/JCDR/2014/10068.5081. Epub 2014 Nov 20. PMID: 25584208; PMCID: PMC4290225.

59. Fowden AL. Insulin deficiency: effects on fetal growth and development. *J Paediatr Child Health*. 1993 Feb;29(1):6-11. doi: 10.1111/j.1440-1754.1993.tb00428.x. PMID: 8461183.

60. Fowden AL. The role of insulin in fetal growth. *Early Hum Dev*. 1992 Jun-Jul;29(1-3):177-81. doi: 10.1016/0378-3782(92)90135-4. PMID: 1396233.

61. Leng S, Zhang W, Zheng Y, Liberman Z, Rhodes CJ, Eldar-Finkelman H, Sun XJ. Glycogen synthase kinase 3 beta mediates high glucose-induced ubiquitination and proteasome degradation of insulin receptor substrate 1. *J Endocrinol*. 2010 Aug;206(2):171-81. doi: 10.1677/JOE-09-0456. Epub 2010 May 13. PMID: 20466847; PMCID: PMC3072280.

62. Hiden, U., Glitzner, E., Hartmann, M. and Desoye, G. (2009), Insulin and the IGF system in the human placenta of normal and diabetic pregnancies. Journal of Anatomy, 215: 60-68. https://doi.org/10.1111/j.1469-7580.2008.01035.x

63. Woods L, Perez-Garcia V, Hemberger M. Regulation of Placental Development and Its Impact on Fetal Growth-New Insights From Mouse Models. *Front Endocrinol (Lausanne).* 2018 Sep 27;9:570. doi: 10.3389/fendo.2018.00570. PMID: 30319550; PMCID: PMC6170611.

64. Tunster, Simon J, Erica D Watson, Abigail L Fowden, and Graham J Burton. "Placental glycogen stores and fetal growth: insights from genetic mouse models". *Reproduction* 159.6 (2020): R213-R235. < https://doi.org/10.1530/REP-20-0007>. Web. 28 Oct. 2022.

65. Mori M, Bogdan A, Balassa T, Csabai T, Szekeres-Bartho J. The decidua-the maternal bed embracing the embryo-maintains the pregnancy. *Semin Immunopathol*. 2016 Nov;38(6):635-649. doi: 10.1007/s00281-016-0574-0. Epub 2016 Jun 10. PMID: 27287066; PMCID: PMC5065593.

66. Borowicz, Pawel P., Arnold, Daniel R., Johnson, Mary Lynn, Grazul-Bilska, Anna T., Redmer, Dale A., Reynolds, Lawrence P., Placental Growth Throughout the Last Two Thirds of Pregnancy in Sheep: Vascular Development and Angiogenic Factor Expression, *Biology of Reproduction*, Volume 76, Issue 2, 1 February 2007, Pages 259–267, https://doi.org/10.1095/biolreprod.106.054684

67. Grazul-Bilska AT, Borowicz PP, Johnson ML, Minten MA, Bilski JJ, Wroblewski R, Redmer DA, Reynolds LP. Placental development during early pregnancy in sheep: vascular growth and expression of angiogenic factors in maternal placenta. *Reproduction*. 2010 Jul;140(1):165-74. doi: 10.1530/REP-09-0548. Epub 2010 Apr 16. PMID: 20400519.

68. Vonnahme KA, Lemley CO, Caton JS, Meyer AM. Impacts of Maternal Nutrition on Vascularity of Nutrient Transferring Tissues during Gestation and Lactation. *Nutrients*. 2015 May 13;7(5):3497-523. doi: 10.3390/nu7053497. PMID: 25984740; PMCID: PMC4446764.

69. Stenhouse C, Hogg CO, Ashworth CJ. Associations between fetal size, sex and placental angiogenesis in the pig. *Biol Reprod*. 2019 Jan 1;100(1):239-252. doi: 10.1093/biolre/ioy184. PMID: 30137229; PMCID: PMC6335214.

70. Cao G, Fehrenbach ML, Williams JT, Finklestein JM, Zhu JX, Delisser HM. Angiogenesis in platelet endothelial cell adhesion molecule-1-null mice. *Am J Pathol*. 2009 Aug;175(2):903-15. doi: 10.2353/ajpath.2009.090206. Epub 2009 Jul 2. PMID: 19574426; PMCID: PMC2716984.

71. Saharinen P, Alitalo K. The yin, the yang, and the angiopoietin-1. *J Clin Invest*. 2011 Jun;121(6):2157-9. doi: 10.1172/JCI58196. Epub 2011 May 23. PMID: 21606600; PMCID: PMC3104784.

72. Egholm C, Khammy MM, Dalsgaard T, Mazur A, Tritsaris K, Hansen AJ, Aalkjaer C, Dissing S. GLP-1 inhibits VEGFA-mediated signaling in isolated human endothelial cells and VEGFA-induced dilation of rat mesenteric arteries. *Am J Physiol Heart Circ Physiol*. 2016 Nov 1;311(5):H1214-H1224. doi: 10.1152/ajpheart.00316.2016. Epub 2016 Sep 16. PMID: 27638877.

73. Holst JJ, Orskov C, Nielsen OV, Schwartz TW. Truncated glucagon-like peptide I, an insulin-releasing hormone from the distal gut. *FEBS Lett*. 1987 Jan 26;211(2):169-74. doi: 10.1016/0014-5793(87)81430-8. PMID: 3542566.

74. Younes ST, Maeda KJ, Sasser J, Ryan MJ. The glucagon-like peptide 1 receptor agonist liraglutide attenuates placental ischemia-induced hypertension. *Am J Physiol Heart Circ*

Physiol. 2020 Jan 1;318(1):H72-H77. doi: 10.1152/ajpheart.00486.2019. Epub 2019 Nov 15. PMID: 31729903; PMCID: PMC6985807.

75. Eastwood MP, Kampmeijer A, Jimenez J, Zia S, Vanbree R, Verbist G, Toelen J, Deprest JA. The Effect of Transplacental Administration of Glucagon-Like Peptide-1 on Fetal Lung Development in the Rabbit Model of Congenital Diaphragmatic Hernia. *Fetal Diagn Ther*. 2016;39(2):125-33. doi: 10.1159/000436962. Epub 2015 Aug 7. PMID: 26277998.

76. Hefetz L, Ben-Haroush Schyr R, Bergel M, Arad Y, Kleiman D, Israeli H, Samuel I, Azulai S, Haran A, Levy Y, Sender D, Rottenstreich A, Ben-Zvi D. Maternal antagonism of Glp1 reverses the adverse outcomes of sleeve gastrectomy on mouse offspring. *JCI Insight*. 2022 Apr 8;7(7):e156424. doi: 10.1172/jci.insight.156424. PMID: 35393955; PMCID: PMC9057621.

77. Gicquel C, Le Bouc Y. Hormonal regulation of fetal growth. *Horm Res*. 2006;65 Suppl 3:28-33. doi: 10.1159/000091503. Epub 2006 Apr 10. PMID: 16612111.

78. Forbes K, Westwood M. The IGF axis and placental function. a mini review. *Horm Res*. 2008;69(3):129-37. doi: 10.1159/000112585. Epub 2008 Jan 8. PMID: 18219215.

79. Sharma D, Farahbakhsh N, Shastri S, Sharma P. Intrauterine growth restriction - part 2. *J Matern Fetal Neonatal Med*. 2016 Dec;29(24):4037-48. doi: 10.3109/14767058.2016.1154525. Epub 2016 Mar 15. PMID: 26979578.

80. Sharma D, Farahbakhsh N, Shastri S, Sharma P. Intrauterine growth restriction - part 2. *J Matern Fetal Neonatal Med*. 2016 Dec;29(24):4037-48. doi: 10.3109/14767058.2016.1154525. Epub 2016 Mar 15. PMID: 26979578.

81. Reynolds LP, Redmer DA. Utero-placental vascular development and placental function. *J Anim Sci*. 1995 Jun;73(6):1839-51. doi: 10.2527/1995.7361839x. PMID: 7545661.

82. Chen DB, Zheng J. Regulation of placental angiogenesis. *Microcirculation*. 2014 Jan;21(1):15-25. doi: 10.1111/micc.12093. PMID: 23981199; PMCID: PMC5589442.

83. Demir R, Seval Y, Huppertz B. Vasculogenesis and angiogenesis in the early human placenta. *Acta Histochem*. 2007;109(4):257-65. doi: 10.1016/j.acthis.2007.02.008. Epub 2007 Jun 15. PMID: 17574656.

84. Ban K, Noyan-Ashraf MH, Hoefer J, Bolz SS, Drucker DJ, Husain M. Cardioprotective and vasodilatory actions of glucagon-like peptide 1 receptor are mediated through both glucagon-like peptide 1 receptor-dependent and -independent pathways. *Circulation*.

2008 May 6;117(18):2340-50. doi: 10.1161/CIRCULATIONAHA.107.739938. Epub 2008 Apr 21. Erratum in: Circulation. 2008 Jul 22;118(4):e81. PMID: 18427132.

85. Almutairi M, Al Batran R, Ussher JR. Glucagon-like peptide-1 receptor action in the vasculature. *Peptides*. 2019 Jan;111:26-32. doi: 10.1016/j.peptides.2018.09.002. Epub 2018 Sep 15. PMID: 30227157.

86. Baggio, Laurie L, Yusta, Bernardo, Mulvihill, Erin E, Cao, Xiemin, Streutker, Catherine J., Butany, Jagdish, Cappola, Thomas P., Margulies, Kenneth B., Drucker, Daniel J., GLP-1 Receptor Expression Within the Human Heart, *Endocrinology*, Volume 159, Issue 4, April 2018, Pages 1570–1584, https://doi.org/10.1210/en.2018-00004

87. Chai, Weidong, Dong, Zhenhua, Wang, Nasui, Wang, Wenhui, Tao, Lijian, Cao, Wenhong, Liu, Zhenqi; Glucagon-Like Peptide 1 Recruits Microvasculature and Increases Glucose Use in Muscle via a Nitric Oxide–Dependent Mechanism. *Diabetes* 1 April 2012; 61 (4): 888–896. https://doi.org/10.2337/db11-1073

88. Di Y, He J, Ma P, Shen N, Niu C, Liu X, Du X, Tian F, Li H, Liu Y. Liraglutide promotes the angiogenic ability of human umbilical vein endothelial cells through the JAK2/STAT3 signaling pathway. *Biochem Biophys Res Commun*. 2020 Mar 12;523(3):666-671. doi: 10.1016/j.bbrc.2020.01.004. Epub 2020 Jan 14. PMID: 31948746.

89. Barut, Figen, Barut, Aykut, Gun, Banu Dogan, Onak Kandemir, Nilufer, Harma, Mehmet Ibrahim, Harma, Muge, Aktunc, Erol, Oguz Ozdamar, Sukru. Intrauterine growth restriction and placental angiogenesis. *Diagn Pathol* **5**, 24 (2010). https://doi.org/10.1186/1746-1596-5-24

90. Ahmed A, Perkins J. Angiogenesis and intrauterine growth restriction. *Baillieres Best Pract Res Clin Obstet Gynaecol*. 2000 Dec;14(6):981-98. doi: 10.1053/beog.2000.0139. PMID: 11141345.

91. Xiao-Yun X, Zhao-Hui M, Ke C, Hong-Hui H, Yan-Hong X. Glucagon-like peptide-1 improves proliferation and differentiation of endothelial progenitor cells via upregulating VEGF generation. *Med Sci Monit*. 2011 Feb;17(2):BR35-41. doi: 10.12659/msm.881383. PMID: 21278683; PMCID: PMC3524715.

92. Kaczynski P, Kowalewski MP, Waclawik A. Prostaglandin F2α promotes angiogenesis and embryo-maternal interactions during implantation. *Reproduction*. 2016 May;151(5):539-52. doi: 10.1530/REP-15-0496. Epub 2016 Feb 23. PMID: 26908918.

93. Stenhouse C, Hogg CO, Ashworth CJ. Associations between fetal size, sex and placental angiogenesis in the pig. *Biol Reprod*. 2019 Jan 1;100(1):239-252. doi: 10.1093/biolre/ioy184. PMID: 30137229; PMCID: PMC6335214.